THE UNIVERSITY OF READING

OPTIMAL STRATEGIES FOR THE CONTROL OF WAVE ENERGY CONVERTERS WITH VARIOUS POWER-TAKE-OFF MECHANISMS

by

N K Nichols & A Crossley

Numerical Analysis Report 3/96

DEPARTMENT OF MATHEMATICS

OPTIMAL STRATEGIES FOR THE CONTROL OF WAVE ENERGY CONVERTERS WITH VARIOUS POWER-TAKE-OFF MECHANISMS

by

N K Nichols & A Crossley

Numerical Analysis Report 3/96

The University of Reading
Department of Mathematics
P O Box 220,
Reading RG6 2AX
Berkshire, UK

This research was supported in part by the Commission for the European Communities under contract CEC JOU2-CT93-0394. This report will appear in Off-Shore Wave Energy Converters (OWEC-1), Annex II: Float Systems and Mathematical Models, CEL DGXII-JOULE II Report, Brussels, 1996.

Optimal Strategies for the Control of Wave Energy Converters with Various Power-Take-Off Mechanisms

N.K. Nichols and A. Crossley

Department of Mathematics
University of Reading
Box 220, Whiteknights
Reading RG6 6AF

Abstract

The aims of this research are to develop and test methods for analysing and computing optimal control strategies for maximizing the useful power *generated* from wave energy converters with realistic power-take-off and control mechanisms. Previously, strategies for maximizing energy *absorbed* by wave devices have been investigated, but these studies have assumed an ideal conversion rate using perfectly efficient turbomachinery with no constraints imposed by the generator capacity. In practice losses occur in the conversion process due to a number of different factors, including mechanical losses in the turbomachinery, head lossses through ducts and limitations on power-take-off. The effect of these losses is nonlinear and depends, in general, on both the hydrodynamic efficiency of the device and on the characteristics of the power-take-off mechanism.

In this report different turbine characteristics and control mechanisms incorporating nonlinear losses are modelled, the qualitative properties of the optimal control strategy for maximizing power delivered at the turbine shaft are analyzed, computational techniques for determining numerical solutions to the optimal control problem are established and the results are tested on a fully developed hydrodynamic model of a wave energy device.

The results confirm that the control gives greater improvement in the energy output for devices that are smaller relative to the wave length. The control of head difference across the turbine is observed to be less robust than the control of turbine flow rate (independent of head difference), and flow rate control strategies that maximize average power *output* are found to be qualitatively different from strategies that optimize energy *absorbed* from the waves.

A significant new result of these studies is that the *improvement* in the generated power produced by optimally controlling the flow rate across the turbine (independently of head difference) *increases with increasing losses* in the turbomachinery.

Contents

1. Summary of Report

1.1 Conclusions

The conclusions are summarized as follows:

1. In order to assess the effectiveness of the device design and the control strategies correctly, realistic models of the power-take-off and control mechanisms need to be incorporated in the device model.

2. Control strategies that maximize the energy *generated* by the power-take-off mechanism are different in nature from the strategies that maximize the energy *absorbed* from the incident wave.

3. The optimal control strategies that maximize energy output where there are losses in the turbo-machinery are not "on-off ", or "bang-bang", but require the turbine flow rate to increase smoothly and shut-off abruptly.

4. Both theoretical analysis and numerical simulation are needed to identify the optimal control strategies. The projected-gradient method is a simple but effective technique for computing the optimal. More robust techniques are available at higher computational cost.

5. Control mechanisms are more effective in improving the power output from devices that are small relative to the average wave length of the sea state than for larger devices. This effect is more pronounced in the case where there are losses in the power-take-off mechanism than where the device is perfectly efficient.

6. The larger the losses in the turbo-machinery, the greater is the improvement in power output that can be achieved by a control mechanism for a device of any size.

7. Control mechanisms using throttle valves to control the head difference across the turbo-machinery are very sensitive. The optimal control problem in this case is ill-conditioned with many local maxima near the optimal. These locally maximal strategies "chatter"; that is, the control oscillates rapidly between closed and open. The "chattering" strategy, in practice, acts to control the flow rate through the turbine. This can be achieved more effectively by a mechanism designed explicitly for this purpose.

8. The effectiveness of the control mechanism is reduced if constraints on the head difference are imposed to prevent the turbine from stalling or choking. As the constraints become stronger, the optimal response approaches that of the uncontrolled system.

9. The use of the turbomachinery as a compressor during part of the wave cycle gives only a small improvement in the average useful power generated by the device model studied here. The improvement is greater for smaller devices relative to a fixed wave length. This improvement is reduced as mechanical losses in the machinery increase, but appears to increase marginally as head losses increase. These effects are likely to be more pronounced if more realistic compressor characteristics are used to model the action of the pump.

10. Further studies are needed to determine optimal control strategies and system responses for specific system devices using sound hydrodynamic models together with the full characteristics of the turbomachinery and the control mechanisms.

1.2. Scope and Objectives

The aims of this project are to develop and test methods for analysing and computing optimal control strategies for maximizing the useful power *generated* from wave energy converters incorporating power-take-off and control mechanisms. Previously, strategies for maximizing energy *absorbed* by wave devices have been investigated, but these studies have assumed an ideal conversion rate using perfectly efficient turbo-machinery with no constraints imposed by the generator capacity.

Specifically, the objectives of the project are to model different turbine characteristics and control mechanisms, to analyze the properties of the optimal control strategy for maximizing power delivered at the turbine shaft, to develop computational techniques for determining numerical solutions to the optimal control problem and to test the results on a fully developed hydrodynamic model of a wave energy device.

1.3. Choice of Methods and Models

The optimal control problem is specified in terms of the power output characteristics of the generating turbine, defined as functions of the flow rate and head difference across the turbine, together with the state equations describing the hydrodynamic response of the device to an incident wave. The flow rate and/or head difference are controlled. The control mechanism is modelled by a non-dimensional control variable with constraints on the range of admissible values.

The analytic techniques used to investigate the optimal control strategy are based on a Maximum Principle derived from the calculus of variations. The standard mathematical theory does not apply directly to wave energy systems due to the convolution integral, representing the wave radiation force, that is contained in the dynamical state equation. A modified theory has been developed previously (Hoskin, Count, Nichols and Nicol, 1986, and Hoskin, 1988) which is used here to treat the optimal wave energy control problem. For constrained problems where the constraints on the control are functions of the state variables of the system, a transformation technique is used to reformulate the problem in terms of controls with fixed constraints, allowing the theory and the numerical procedures to be applied to these cases.

The primary computational method used to determine the numerical solutions to the optimal control problem is a simple but efficient discretized projected-gradient technique. As a class the gradient-type methods have fast rates of convergence and the projected-gradient algorithm, in particular, proves to be effective in treating the class of problems which arise in the modelling of power-take-off mechanisms in wave energy devices. Conditional gradient algorithms have been used previously and are more suitable for computing "on-off " control strategies, but as shown by the analysis, the optimal controls for systems containing realistic turbine characteristics are not strictly "on-off" strategies and the projected-gradient algorithm is found to provide more satisfactory results for the models formulated here. The discretized form of the projected-gradient method is not highly robust, however, and for extremely sensitive, or ill-conditioned, optimal control problems an alternative approach is used. In such cases, the control problem is completely discretized and a sophisticated discrete optimization package is applied (Conn, Gould and Toint, 1992). This approach is more robust than the simpler projected-gradient method but requires much greater computational power.

A time-domain model of an oscillating water column wave energy converter equipped with a Wells type turbine is used in this investigation. The model was developed under the EC JOULE I R&D Programme and a numerical simulator was constructed (Justino, Nichols and Falcão, 1993). The

model combines a good hydrodynamic description of the device with a facility for incorporating various power-take-off and control mechanisms in the simulator and was selected as it was fully developed at the start of this project The analytic conclusions obtained with this model are generic, however, and the techniques developed in this study can readily be applied to other device models. The hydrodynamics of the system need to be modelled accurately, however, for the conclusions to be valid, as shown in the float system study completed as part of this project (Greenhow and White, 1996).

1.4. Methodology

Details of the modelling and the analytical and numerical techniques used in this research are described in the main sections of the report. The mathematical formulations of the device model, the turbine characteristics and the control mechanisms are derived in Section 2. The optimal control problem is specified in Section 3 and qualitative properties of the optimal control strategies are investigated. The complete discretized algorithm for computing the numerical solutions to the optimal control problem is then defined in Section 4.

1.5. Results

1.5.1 Analytical Results

Results of the analysis show that the optimal form of the control strategy depends on the type of control mechanism used.

If the head difference across the turbine is controlled, through a throttle valve for example, the optimal strategy for a perfectly efficient power-take-off mechanism (designed to maximize power *absorbed* from the incident wave) is an "on-off " strategy. This property still holds if there are losses in the turbomachinery.

If the flow rate is controlled, by a variable geometry turbine for example, then the optimal strategy also appears to be "on-off " for perfectly efficient turbines, but now "singular arcs" can arise in the solution to the optimization problem and interior values of the control may be maximizing. For power-take-off mechanims with losses, the optimal strategies for flow rate control are no longer "on-off ", but require the flow rate to increase smoothly between prescribed limits, as the turbine is brought on-line, and to shut off abruptly.

If the flow rate is controlled indirectly by a relief or by-pass valve, the analysis shows that the optimal control is an "on-off" strategy and cannot contain singular arcs.

1.5.2 Numerical Results

The numerical results confirm the analytical results.

In the case where the head difference across the turbine is controlled, the optimization problem is found to be ill-conditioned and to have many local maxima near the optimal. The numerical solutions are highly sensitive to the initial approximation used in the computational iteration procedures and it is, therefore, very difficult to determine the optimal accurately. The locally maximal strategies "chatter"; that is, the control oscillates between off and on at every discrete point over some part of the wave cycle. The onset and length of the chattering period is also numerically

sensitive. This behaviour can be understood from the results obtained in the case where the flow rate is controlled. The "chattering" strategy can be seen to act in practice to control the flow rate through the turbine smoothly.

In the case where the flow rate is controlled directly, the numerical results show that the optimal strategy for a perfectly efficient power-take-off mechanism does contain "singular arcs," as predicted by the analysis. The optimization problem, although still mildly sensitive, can be solved relatively easily to the desired accuracy. Along the singular arcs, the gradient of the power functional is zero and the control is determined implicitly by this condition. The optimal control is observed to increase relatively smoothly between its prescribed limits along the singular arcs. These periods correspond to periods of chattering in the case where the head difference is controlled, and the chattering control can be interpreted as giving a "bang-bang" approximation to the required optimal flow rate strategy. A mechanism designed explicitly to control the flow rate is expected, therefore, to be more effective and more robust than a mechanism that controls the flow rate implicitly by controlling the head difference.

For power-take-off mechanisms with losses, this conclusion is even more clear. In this case the optimal strategy for controlling the head difference remains "on-off ", or "bang-bang." In contrast, the optimal strategy for controlling the flow rate now contains interior segments that are explicitly defined and the optimal control varies smoothly along these segments.

In the case where a by-pass or relief valve is used implicitly to control the flow, the numerical results exhibit the "on-off" behaviour predicted by the analysis, without any chattering of the valve.

Detailed results of experiments with regular incident waves of different lengths, for optimally tuned devices of different sizes, equipped with various power-off-take and control mechanisms are discussed in Section 5 of the report. The optimal strategies and corresponding system responses are shown for various cases in the attached Figures. The effectiveness of the optimal strategies under various conditions is demonstrated in the Tables, which show the ratio of the optimally controlled power output to the uncontrolled output. In evaluating the results it should be recognized that the device model used here is already well-tuned to the wave climate, and that the gains that can be achieved by controlling the system are not great. For smaller devices, or longer sea waves, the effectiveness of the controls increases greatly, as can be seen from some of the Tables. Conclusions that can be drawn from these experiments are summarized in Section 1.1.

2. Mathematical Models

In this section we discuss the aims of the research and specify the device models, including the turbine characteristics and control mechanisms, that are used in the investigation.

2.1 Background

Previous research has mainly concentrated on optimizing device designs with respect to the energy *absorbed* from the wave, assuming a perfectly efficient power conversion mechanism. Optimal damping and stiffness characteristics of the converter have been identified for regular wave conditions using frequency domain analysis. Control mechanisms for increasing absorbed energy from various devices in non-resonant wave conditions have been proposed and investigated. The aim

of the control strategies has been to bring the device velocity into phase with the incident wave diffraction force, thereby reducing losses in absorbed energy.

Two types of control strategy have been investigated: *latching strategies* and *reactive loading strategies*. Latching is achieved by physically halting the device motion in the case of float systems or by stopping the air flow to the converter in the case of pneumatic devices. Theoretically, latching enables the attainment of energy absorption close to the maximum achievable with linear mechanical conditioning in regular waves. Through simulation studies, latching mechanisms have also been shown to lead to improved energy absorption over the whole sea-spectrum. Reactive loading, in contrast to latching strategies, allows the flow rate and head difference across the turbine to be controlled independently. With such control mechanisms the theoretical maximal energy absorption can be attained for any wave profile. Perfect reactive loading in this case requires the reverse operation of the power converter, however, so that during parts of the wave cycle, energy must be pumped into the system.

The improvement in energy absorption resulting from the application of a control mechanism has been shown to depend on the size of the device and the frequency range of the local wave climate. It has been established that efficient energy absorption over a wider frequency band is enabled by a controller and that control mechanisms are most effective for improving the productivity of relatively small devices. Controllers thus allow the use of smaller plants for the same gains and enable the delivered cost of the energy to be reduced. (See Nichols, 1993, for references.)

It has been demonstrated, however, that control strategies that optimize energy absorption are not equivalent to strategies that maximize the useful power *generated* by wave energy converters under operational conditions (Sarmento, Gato and Falcão, 1990; Nichols, Falcão and Pontes, 1991). Losses occur in the conversion process due to a number of different factors, including mechanical losses in the turbomachinery, head lossses through ducts and limitations on power-take-off. The effect of these losses is nonlinear and depends, in general, on both the hydrodynamic efficiency of the device and on the characteristics of the power-take-off mechanism. For the optimization and evaluation of device designs it is necessary, therefore, to investigate models of the devices that incorporate realistic characteristics of the conversion and control mechanisms.

The aims of this research project are to develop and test techniques for analysing and computing optimal control strategies for maximizing power output from wave energy devices with specified power conversion mechanisms. A basic framework for investigating the optimal control problem is provided by the calculus of variations and Pontryagin's Maximum Principle. Analysis is carried out in the time-domain, using mathematical models of the device. Qualitative properties of the optimal strategy are derived from the necessary conditions for the optimal, and discrete numerical optimization techniques are applied to compute solutions to the control problem.

Specifically, the objectives of the project are to model different turbine characteristics and control mechanisms, to analyze the properties of the optimal control strategy for maximizing power delivered at the turbine shaft, to develop computational techniques for determining numerical solutions to the optimal control problem and to test the results on a fully developed hydrodynamic model of a wave energy device. In the next three sections, the device model used in this investigation is defined and models of the power-take-off and control mechanisms are developed. In the following main sections of the report the optimal control problem is formulated and analyzed for various system models and the numerical techniques used to solve the optimization problem are described. Numerical results and conclusions are presented in the final sections of the report.

2.2 Device Model

In this project we investigate an oscillatory water column (OWC) wave energy converter. A time domain model for this device was developed under the previous EC JOULE R&D Programme and a numerical simulator was constructed. This model combines a good hydrodynamic description of the device with a facility for incorporating realistic power-take-off mechanisms. The device is assumed to be fixed with respect to the sea bed, which is taken to be of arbitrary depth and shape. The waves incident upon the device are supposed in general to be irregular. The analysis is based on classical linear water-wave theory and follows that of Nichols, Falcão and Pontes (1991).

We let $p(t)+p_a$ be the air pressure (assumed uniform) inside the chamber, where p_a is atmospheric pressure, and let $q_c(t)$ be the volume flow rate displaced by the internal free surface of the water in the chamber ($q_c > 0$ for upward motion). The flow rate of the volume $V(t)$ of air in the chamber is then $dV/dt = -q_c$, and the mass flow rate $-dm/dt$ through the turbine (positive for outward flow) can be written

$$-\frac{dm}{dt} = -\frac{d}{dt}(\rho V) = -V\frac{d\rho}{dt} + \rho q_c . \tag{2.1}$$

The relationship between the pressure and the density ρ of air depends on the thermodynamic process taking place inside the chamber and the turbine. (See Falcão and Justino, 1994). Here we consider the air to be a perfect gas and assume that both the discharging and filling processes are isentropic. Consequently we may write

$$(p+p_a)\rho^{-\gamma} = \text{constant} = p_a\rho_a^{-\gamma} \tag{2.2}$$

where ρ_a is the atmospheric air density and $\gamma = c_p/c_v$ is the specific heat ratio. In addition, the variation in air density is considered small, that is, $|\rho - \rho_a| << \rho_a$, which allows us to write density as a linear function of pressure

$$\rho = \rho_a\left[1 + \frac{p(t)}{\gamma p_a}\right]. \tag{2.3}$$

If we assume also that $|V - V_o| << V_o$, where V_o is the volume of the air chamber at equilibrium, then the volume flow rate q through the turbine can be written as

$$q(t) \equiv -\frac{1}{\rho_a}\frac{dm}{dt} = -\frac{V_o}{\gamma\rho_a}\frac{dp}{dt} + q_c(t). \tag{2.4}$$

The flow rate $q_c(t)$ can be decomposed using linear water-wave theory in the form

$$q_c(t) = q_r(t) + q_d(t), \tag{2.5}$$

where q_r is the radiation flow rate induced by air pressure oscillation in the chamber in the absence of incident waves and q_d is the diffraction flow rate due to the incident wave field with the air chamber held at atmospheric pressure.

Within the framework of linear water wave theory, the radiation flow can be expressed in the form

$$q_r(t) = \int_o^\infty \kappa(\tau) p(t-\tau) d\tau = \int_{-\infty}^t \kappa(t-\tau) p(\tau) d\tau \,, \tag{2.6}$$

where $\kappa(\tau)$ depends on the geometry of the system. This function is easily related to the system's radiation coefficient by setting $p(t) = \hat{P} e^{i\omega t}$, $q_r(t) = \hat{Q}_r e^{i\omega t}$, where $\hat{P}(\omega)$, $\hat{Q}_r(\omega)$ are in general complex. The complex coefficient of radiation is by definition (Evans, 1982) $B(\omega) + iC(\omega) = \hat{Q}_r(\omega) / \hat{P}(\omega)$, where B, C are real. Assuming $\kappa(\tau)$ to be an even function, we find by a Fourier transform that

$$B(\omega) = \tfrac{1}{2} \int_{-\infty}^\infty \kappa(t) e^{-i\omega t} dt \,, \tag{2.7}$$

from which, by inversion, we obtain

$$\kappa(t) = \frac{2}{\pi} \int_o^\infty B(\omega) \cos(\omega t) d\omega \,. \tag{2.8}$$

The function $B(\omega)$ depends on the geometry of the device and is assumed to be known either theoretically or from measurements.

Combining equations (2.4), (2.5) and (2.6) we obtain

$$\frac{dp}{dt} = -cq(t) + c \int_o^t \kappa(t-\tau) p(\tau) d\tau + cq_d(t), \tag{2.9}$$

where $c = \gamma p_a / V_o$ and we assume, without loss of generality, that $p = 0$ for $t \le 0$. The turbine flow rate $q(t)$ is determined by the power take-off and control mechanisms, and for a given incident wave form the diffraction flow rate $q_d(t)$ is assumed to be a known function of time, dependent on the geometry of the device.

In the numerical simulator a simple two-dimensional geometry is adopted for the device. The incident waves are assumed to propagate unidirectionally towards the device along a channel of constant depth h and of constant width b equal to the inner chamber width. This geometry can be regarded as an approximation to an OWC device built in a gulley (such as the pilot plants designed for Islay in Scotland and Pico in the Azores). The chamber consists of a vertical fully reflecting back wall and a front wall at distance a from the back wall. It is assumed that the lower lip of the front wall is submerged to a negligible depth and is of small thickness, so that the diffraction it produces may be ignored.

For this geometry the hydrodynamic coefficient of radiation $B(\omega)$ is given analytically (Sarmento and Falcão, 1985) by

$$B(\omega) = -\frac{2\omega\mu b}{\rho_w g k} \sin^2 ka \,, \tag{2.10}$$

where g is the acceleration of gravity, ρ_w is the density of water, k is the wave number, related to

the angular frequency ω by the dispersion relationship

$$k \tanh kh = \omega^2 / g, \tag{2.11}$$

and $\mu = (1 + (\omega^2 / g) h \cosech^2(kh))^{-1}$. The procedure for computing $\kappa(t)$, defined by (2.8), is described in (Justino, 1993). It should be noted that $\kappa(t)$ has a logarithmic singularity at $t = 0$ which is integrable.

If the diffraction due to the front wall is neglected, then the diffraction flow rate q_d is simply that of the volume displaced inside the chamber by the free surface of the stationary wave system, which is obtained from the superposition of the incident wave and the wave reflected from the back wall. For a regular incident wave with angular frequency ω and amplitude $\mathcal{A}$, we find that

$$q_d(t) = \frac{2b\mathcal{A}\omega}{k} \sin(2ka) \cos(\omega t + \theta), \tag{2.12}$$

where θ is the (random) phase shift. The energy flux of the incident wave, equal to the rate of work done by the pressure forces on a vertical plane at a fixed point in the channel, averaged over an integer number of wave periods is given by

$$E_f = \mathcal{A}^2 b \rho_w g \omega / 4 \mu k. \tag{2.13}$$

Regular waves are simulated by the superposition of a finite number N of regular waves. The diffraction flow rate is then

$$q_d = 2b \sum_{j=1}^{N} \frac{\mathcal{A}_j \omega_j}{k_j} \sin(2k_j a) \cos(\omega_j t + \theta_j), \tag{2.14}$$

where it is assumed that $\omega_j = \omega_o / N_j$, N_j an integer. The average energy flux of the composite wave over the wave period is then given by

$$E_f = \frac{b \rho_w g}{4} \sum_{j=1}^{N} \frac{\mathcal{A}_j^2 \omega_j}{\mu_j k_j}. \tag{2.15}$$

The spectral distribution of the irregular waves is taken to be representative of the wave climate measured at the pilot plant site on Pico in the Azores.

2.3 Turbine Characteristics

From turbomachinery theory it is known that the mass flow rate dm/dt through the turbine depends on the pressure difference p_t across the turbine and on the rotational speed Ω of the turbine, as well as on the stagnation conditions at the turbine entrance (that is, on p_a, ρ_a for inward flow and p, ρ for outward flow). Here we may ignore the effects of varying inlet stagnation conditions, since we assume that pressure and density variations are small compared to p_a, ρ_a. The volumetric flow

rate q through the turbine can then be expressed in the form

$$q = \Omega\Phi\left(\frac{p_t}{\Omega^2}\right). \tag{2.16}$$

For a Wells type turbine, which is known to be linear in characteristic, the volumetric flow rate can be written

$$q = K' p_t / \Omega, \tag{2.17}$$

where K' depends upon ρ_a and the diameter of the turbine.

The power P generated at the turbine shaft is also a function of both the pressure difference p_t across the turbine and the rotational speed Ω and can be expressed in the form

$$P = \Omega L_t(p_t, \Omega) \equiv \Omega^3 \Pi\left(\frac{p_t}{\Omega^2}\right), \tag{2.18}$$

where $L_t \equiv \Omega^2 \Pi$ is the turbine torque. In the case where there are no losses in the turbo-machinery, and all the energy available to the turbine is output, we have

$$P = P_A \equiv q p_t, \tag{2.19}$$

which for a Wells type turbine implies that the function Π is given by

$$\Pi = K'\left(\frac{p_t}{\Omega^2}\right)^2. \tag{2.20}$$

In the case where there are losses, we have $P = q p_t \eta_t$, where η_t is defined to be the turbine efficiency. The efficiency may be expressed in terms of the power losses $\mathcal{L}$ in the form $\eta_t = 1 - \mathcal{L} / P_A$. A simple approximation to the power losses in the Wells type turbine can be written

$$\mathcal{L} = \Omega D q^2 + \Omega^3 C. \tag{2.21}$$

The power output is then given by (2.18) where

$$\Pi = K'(1 - DK')\left(\frac{p_t}{\Omega^2}\right)^2 - C. \tag{2.22}$$

In practice, the function Π is adequately approximated by a quadratic function of the form

$$\Pi(\xi) = a_2 \xi^2 + a_1 |\xi| - a_o, \tag{2.23}$$

where $\xi = p_t / \Omega^2$ and $a_2, a_1, a_o > 0$.

For a given characteristic curve Π, the turbine operates at maximum *efficiency* where the rotational speed Ω_E of the turbine is related to the pressure p_t across the turbine by the equation

$$\Omega_E = \sqrt{p_t / \xi_E}\,. \tag{2.24}$$

Here ξ_E is a dimensionless quantity satisfying

$$\frac{\partial P}{\partial \Omega} = \frac{\partial}{\partial \Omega}(\Omega^3 \Pi(\xi)) = 3\Omega^2 \Pi - \frac{2}{3}\xi \Omega^3 \Pi' = 0\,, \tag{2.25}$$

or equivalently,

$$\frac{2}{3}\xi_E \Pi'(\xi_E) = \Pi(\xi_E). \tag{2.26}$$

For some types of turbine, including in particular the Wells type turbine, the curve $\Pi(\xi)$ exhibits a maximum for a critical value $|\xi| = \xi_{cr}$. It is undesirable to operate the turbine at values of $\xi = p_t / \Omega^2$ beyond the critical value, as power is lost and stalling or choking of the turbine can result. In practice a control mechanism, such as a by-pass relief valve or a throttle valve in the turbine duct, is used to prevent the critical value being exceded.

For a two-dimensional device with the geometry described in Section 2.2, equipped with a Wells type turbine operating at a fixed rotational speed Ω and driven by a regular incident wave of frequency ω, an optimal value for the turbine constant $K = K' / \Omega$ is given by Sarmento and Falcão (1985). The optimal parameter maximizes the proportion of the available energy E_f that is absorbed by the device from the wave. Maximum absorption of 100% can be achieved for complex values of K; for such parameters the turbine is operating out of phase with the flow and must act, over part of the cycle, as a compressor, supplying energy to the wave field. For the models examined here, no phase difference is assumed, and K is selected to be real and such as to maximize energy absorption at a typical wave frequency in the sea spectrum. The control mechanisms can be used, however, to enable the turbine to act as a compressor over parts of the wave cycle.

2.4 Control Mechanisms

Three basic mechanisms for controlling the device are available. The first allows for the pressure p_t across the turbine to be controlled using a throttle valve. The second permits flow through the turbine to be controlled, for example, by a variable geometry turbine. The third is a by-pass or relief valve.

2.4.1 Control of Pressure Difference

We assume that the rotational speed Ω of the turbine is fixed at a constant value Ω_1 and that the pressure p_t can be controlled. In the simplest model we take p_t to be directly proportional to the

pressure p and write

$$p_t = \alpha p, \qquad \alpha \in [0,1], \tag{2.27}$$

where $\alpha(t)$ is a (non-dimensional) control variable. To ensure that p_t does not exceed the critical value $p_{cr} \equiv \Omega_1^2 \xi_{cr}$ for the turbine, we need to limit the control $\alpha(t)$ to satisfy

$$\begin{aligned} &\alpha \in [0,1] \qquad \text{for } |p| \le p_{cr}, \\ &\alpha \in [0, p_{cr}/|p|] \quad \text{for } |p| \le p_{cr}. \end{aligned} \tag{2.28}$$

A more sophisticated model can be obtained by assuming that p_t is controlled via a throttle valve. Then we find

$$p_t = p - \tilde{\alpha}^2 \left(\frac{\rho_a}{2A^2} \right) \sigma q^2 \tag{2.29}$$

where $\sigma = sign(p)$, A is a reference area related to the turbine diameter, and $\tilde{\alpha}(t)$ is now the (non-dimensional) control variable. Substituting into (2.29) for $q = Kp_t$ from (2.17), where $K = K'/\Omega_1$, we obtain

$$p_t = \frac{\sigma}{2\tilde{\alpha}^2 \nu^2} (-1 + \sqrt{1 + 4\tilde{\alpha}^2 \nu^2 |p|}) \tag{2.30}$$

with $\nu^2 = \rho_a K^2 / 2A^2$. Assuming ν^2 is sufficiently small, we find that a reasonable approximation to p_t is given by

$$p_t = p - \tilde{\alpha}^2 \nu^2 p|p|. \tag{2.31}$$

The limits on the control variable are now

$$0 \le \tilde{\alpha} \le 1/(\nu\sqrt{|p|}) \tag{2.32}$$

For $\tilde{\alpha} = 0$, the valve is fully open and $p_t = p$. For $\tilde{\alpha}$ at its maximum value, the pressure difference p_t across the turbine becomes zero. To ensure that p_t does not exceed the critical value for the turbine, we limit $\tilde{\alpha}$ to satsify (2.32) for $|p| \le p_{cr}$ and

$$\frac{1}{\nu|p|}\sqrt{|p| - p_{cr}} \le \tilde{\alpha} \le \frac{1}{\nu|p|} \qquad \text{for } |p| \ge p_{cr}. \tag{2.33}$$

Although this model appears more realistic than the simple model initially proposed, from an analytic point of view, the optimal control strategies reduce to the same form. Indeed, $\tilde{\alpha}^2$ can be generated directly from α using $\tilde{\alpha}^2 = (1-\alpha)/(\nu\sqrt{|p|})$.

2.4.2 Control of Flow Rate

In the simplest model of flow control, we assume that the flow rate q across the turbine can be

controlled, independently of the pressure, proportionally between zero and the maximum capacity of the turbine; that is, we take

$$q = \alpha K p_t \tag{2.34}$$

where $K = K'/\Omega_1$, Ω_1 is a nominal value of the roational speed of the turbine, and the (non-dimensional) control variable $\alpha(t)$ satisfies

$$\alpha(t) \in [0,1]. \tag{2.35}$$

If no pressure losses are assumed in the turbomachinery, then $p_t = p$. Alternatively losses may be modelled as for a throttle valve. In this case

$$p_t = p - \left(\frac{\rho_a}{2A^2}\right)\sigma q^2 \tag{2.36}$$

where A is some representative area and $\sigma = sign(p)$. Substituting for q from (2.34) and solving for p_t gives (2.30) as before. Provided that $\nu^2 = \rho_a K^2/(2A^2)$ is sufficiently small, p_t can be approximated as in (2.31), and we find that the controlled flow rate is given as a function of p by

$$q = K\alpha(p - \alpha^2 \nu^2 p|p|). \tag{2.37}$$

If we allow the turbine to act as a compressor during part of the wave cycle, then the flow can be driven in the opposite direction to the pressure difference, and the control $\alpha(t)$ may take negative values. In this simple model we restrict α to the range

$$\alpha(t) \in [-1,1], \tag{2.38}$$

and assume that the turbine characteristics are the same for both compression and generation modes. More sophisticated models can be constructed that allow for different characteristics in each mode of operation (Andrews, Nichols and Xu, 1990).

To ensure that the critical turbine flow is not exceeded at the rotational speed Ω_1 we require that $|\alpha(t)|$ satisfies

$$\begin{aligned} &|\alpha(t)| \in [0,1] && \text{for } |p_t| \le p_{cr} \equiv \Omega_1^2 \xi_{cr}, \\ &|\alpha(t)| \in [0, p_{cr}/|p_t|] && \text{for } |p_t| \ge p_{cr}. \end{aligned} \tag{2.39}$$

In practice, the flow is controlled independently of the pressure, and the pressure p_t across the turbine cannot be maintained below its critical level for a given rotational speed by controlling the turbine flow alone. An additional control mechanism is needed.

2.4.3 Control of Relief Valve

An alternative mechanism for controlling the flow rate is a by-pass or relief valve. The total volumetric flow rate q is then given by the sum of the flow rate q_t through the turbine and the flow rate q_v through the valve. The valve flow rate is given by

$$q_v = \tilde{\alpha} A \sigma \sqrt{\frac{2|p|}{\rho_a}} \tag{2.40}$$

where the (non-dimensional) control variable $\tilde{\alpha}(t) \in [0,1]$, $\sigma = sign(p)$ and A is some representative area. The total flow then takes the form

$$q = q_t + \tilde{\alpha} \beta \sigma \sqrt{|p|} \tag{2.41}$$

where $\beta = A\sqrt{2/\rho_a}$.

In this case, to ensure that $q_t = Kp_t$ does not exceed the critical value at the rotational speed Ω_1, we require that for $|p_t| \geq p_{cr} \equiv \Omega_1^2 \xi_{cr}$,

$$0 \leq \tilde{\alpha} \leq (|\tilde{q}| - Kp_{cr}) / (\beta \sqrt{p_{cr}}) \tag{2.42}$$

where $\tilde{q}$ is the total flow rate needed to ensure that $|p_t| = p_{cr}$ is maintained; that is, $\tilde{q}$ is such that $dp/dt = 0,$, where dp/dt is given by (2.9) with $q = \tilde{q}$.

In practice the two flow control mechanisms described in Sections 2.4.2 and 2.4.3 need to be used together to achieve the desired behaviour of the system.

3. Optimal Control Strategies

The optimal control problem is to determine the control strategy that maximizes the *generated* energy E produced by the wave plant during a given time interval $0 \leq t \leq T$, subject to the dynamical system equations and the constraints on the control (and state) variables being satisfied. We observe that the optimal strategy for maximizing the average power *absorbed* by the device from the wave is not in general the same as the optimal strategy that maximizes the average useful power *produced* by the plant via the turbomachinery.

For the models described here, the optimal control problem can be written

$$\underset{\alpha}{\text{maximize}} \; E \equiv \int_0^T P(\alpha, p) dt \tag{3.1}$$

subject to

$$\dot{p} = -cq(\alpha, p) + c\int_0^t \kappa(t-\tau) p(\tau) d\tau + cq_d(t), \quad p(0) = 0, \tag{3.2}$$

and

$$\alpha_{\min} \le \alpha \le \alpha_{\max}, \tag{3.3}$$

where we have assumed, without loss of generality, that $p(t) \equiv 0$ for $t \le 0$, and that the volumetric flow rate q and the instantaneous power output P are given functions of the control variable α and the state variable p. The bounds $\alpha_{\min}$, $\alpha_{\max}$ on the control variable may also be explicitly dependent on the state p.

Following the arguments used in Hoskin, Count, Nichols and Nicol (1986), Hoskin (1988) and Andrews, Nichols and Xu (1990), based on the calculus of variations, we can obtain necessary conditions for an optimal control α^* and its corresponding optimal state p^* to solve the problem (3.1)-(3.3). In the case where the bounds $\alpha_{\min}$, $\alpha_{\max}$ are independent of the state p, we find that the optimal solution must satisfy equations (3.2)-(3.3) together with an adjoint equation

$$\dot{\lambda} = c\lambda\alpha \frac{\partial q}{\partial p} - c\int_t^T \kappa(\tau - t)d\tau - \frac{\partial P}{\partial p}, \qquad \lambda(T) = 0, \tag{3.4}$$

and a Maximum Principle, expressed by

$$H(\alpha^*, p^*, \lambda) \equiv \max_{\alpha_{\min} \le \alpha \le \alpha_{\max}} H(\alpha, p^*, \lambda), \tag{3.5}$$

where

$$H(\alpha, p, \lambda) \equiv P(\alpha, p) + \lambda(-cq(\alpha, p) + c\int_0^t \kappa(t - \tau)p(\tau)d\tau + cq_d(t)).$$

In the case where the constraints on the control depend explicitly on the state, a transformation on the control variable is first used to eliminate the dependency of the bounds $\alpha_{\min}$, $\alpha_{\max}$ on p. The necessary conditions then follow by applying the theory to the modified problem.

The form of the optimal controller can be deduced from the Maximum Principle (3.5). In the following subsections we examine the behaviour of the optimal solution under different assumptions on the turbine characteristics and the control mechanisms.

3.1 Control of Perfectly Efficient Devices

We first consider cases where all of the energy available to the turbine is output; that is, the turbomachinery is perfectly efficient (with $\eta_t = 1$) and the power generated by the turbine is given by $P = P_A \equiv qp_t$.

3.1.1 Optimal Control of Pressure Difference

In the simplest model of pressure control we assume that p_t can be controlled proportionately to the pressure p in the chamber and therefore that $p_t = \alpha p$, where $\alpha \in [0,1]$. The flow is then given

by $q = Kp_t$ and the available power is $P_A = K\alpha^2 p^2$. For α^* to be optimal, the Maximum Principle (3.5) then implies that

$$K\alpha^2 p^2 - \lambda c K\alpha p \equiv K\alpha p(\alpha p - \lambda c) \tag{3.6}$$

must be maximized by α^*. It follows directly that the optimal occurs where α takes either its maximum or minimum value and hence

$$\begin{aligned} \alpha^* &= 0 \quad \text{if } p(p-\lambda c) < 0 \\ &= 1 \quad \text{otherwise.} \end{aligned} \tag{3.7}$$

We observe also that

$$H_\alpha \equiv \frac{\partial H}{\partial \alpha} = Kp(2\alpha p - \lambda c) = 0 \tag{3.8}$$

where $\alpha = \alpha_m = (p - \lambda c)/2$. At this point, however

$$H_{\alpha\alpha} \equiv \frac{\partial^2 H}{\partial \alpha^2} = 2Kp^2 \geq 0 \tag{3.9}$$

and hence α_m *minimizes* the Hamiltonian (3.6) and does not give an optimal strategy.

If we constrain α to satisfy $\alpha \in [0, p_{cr}/|p|]$ in order to ensure that the turbine pressure does not exceed its critical value, then we must modify the problem before applying the necessary conditions. We make the transformation $\alpha = uG(p)$ where

$$\begin{aligned} G(p) &= 1 \quad \text{if } |p| \leq p_{cr} \\ &= p_{cr}/|p| \quad \text{if } |p| \geq p_{cr}, \end{aligned} \tag{3.10}$$

and require $u \in [0,1]$. The pressure is then given by $p_t = upG(p)$ and $q = Kp_t$, $P_A = qp_t = Ku^2 p^2 G^2(p)$. Applying the theory to the modified problem, we find that the optimal α^* takes the form

$$\begin{aligned} \alpha^* = u^* G(p) \quad &= 0 \quad \text{if } pG(p)[pG(p) - \lambda c] < 0, \\ &= G(p) \quad \text{otherwise.} \end{aligned} \tag{3.11}$$

If we consider the more sophisticated model where p_t is controlled via a throttle valve, then essentially the same results hold. Ignoring higher order terms in p_t, we have

$$p_t = p - \tilde{\alpha}^2 \nu^2 p|p|, \qquad q = Kp_t, \tag{3.12}$$

and, therefore,

$$P_A = Kp_t^2 = K(p^2 - 2\tilde{\alpha}^2\nu^2 p^2|p| + \alpha^4 \nu^4 p^4), \tag{3.13}$$

where

$$\tilde{\alpha} \in [0,1/(\nu\sqrt{|p|})]. \tag{3.14}$$

We may use the same technique as previously to transform $\tilde{\alpha}$ onto a fixed interval, independent of the state p, and then apply the optimality conditions. We find that the optimal $\tilde{\alpha}^*$ must now maximize

$$K\tilde{\alpha}^2\nu^2p^2(\tilde{\alpha}^2\nu^2p^2 - \sigma(2p-\lambda c)), \tag{3.15}$$

where $\sigma = sign(p)$, and, therefore,

$$\begin{aligned} \tilde{\alpha}^* &= 1/(\nu\sqrt{|p|}) \quad \text{if} \quad \sigma(p-\lambda c) < 0, \\ &= 0 \qquad\qquad\quad \text{otherwise.} \end{aligned} \tag{3.16}$$

We find also that

$$H_{\tilde{\alpha}} = K2\tilde{\alpha}^2\nu^2p^2(2\tilde{\alpha}^2\nu^2p^2 - \sigma(2p-\lambda c)) = 0 \tag{3.17}$$

at

$$\tilde{\alpha}^2 = \sigma(2p-\lambda c)/(2\nu^2p^2), \tag{3.18}$$

which gives a real value for $\tilde{\alpha}$ provided $\sigma(2p-\lambda c) > 0$. For this value of $\tilde{\alpha}$, however, $H_{\tilde{\alpha}\tilde{\alpha}} > 0$ and hence (3.18) does not give a maximizing value for the control.

These results are to be expected, since there is a direct correspondence between $\tilde{\alpha}$ and the control α for the simple model, as shown in Section 2.4. In the case where we require $|p_t| \le p_{cr}$, this correspondence can be used to find the optimal strategy $\tilde{\alpha}^*$ directly from (3.11). We find that

$$\begin{aligned} \tilde{\alpha}^* &= 1/(\nu\sqrt{|p|} \qquad\qquad \text{if} \quad \sigma(\rho - \lambda c) < 0, \\ &= 0 \qquad\qquad \text{if} \quad \sigma(\rho - \lambda c) > 0 \text{ and } |p| \le p_{cr}, \\ &= \frac{1}{\nu|p|}\sqrt{|p| - p_{cr}} \qquad \text{otherwise.} \end{aligned} \tag{3.19}$$

The optimal strategy for controlling the pressure is thus a 'bang-bang' strategy in all cases, and no interior control strategy is maximizing.

3.1.2 Optimal Control of Turbine Flow Rate

We now examine the optimal strategies for controlling the flow in the case of a perfectly efficient turbine where there are no pressure losses in the machinery. For the simple model we have $p_t = p$ and

$$q = \alpha Kp, \quad P \equiv P_A = \alpha Kp^2 \tag{3.20}$$

where $\alpha \in [0,1]$. The Maximum Principle (3.5) then implies that

$$K\alpha p^2 - \lambda c K\alpha p \equiv \alpha p(p - \lambda c)$$

must be maximized by α^*. It again follows that α^* must satisfy

$$\begin{aligned} \alpha^* &= 0 \quad \text{if } p(p - \lambda c) < 0 \\ &= 1 \quad \text{otherwise.} \end{aligned} \tag{3.21}$$

It appears, therefore, that the strategies for controlling the flow and the pressure are the same in the simplest cases. If we examine the gradient of the Hamiltonian, we find now, however, that

$$H_\alpha = p(p - \lambda c), \tag{3.22}$$

which is independent of α. It is thus possible that $H_\alpha \equiv 0$ over some interval of time. In this case the control α is determined implicitly by (3.22) together with the state and adjoint equations (3.2) and (3.4), respectively. For such a control to be maximizing the Clebsh condition (Bryson and Ho, 1975)

$$(-1)^m \frac{\partial}{\partial \alpha}\left[\frac{d^{2m}}{dt^{2m}} H_\alpha\right] \leq 0 \tag{3.23}$$

must hold for the first positive integer m where $d^{2m}H_\alpha / dt^{2m}$ depends non-trivially on α. Here $H_\alpha \equiv 0$ implies that either (i) $p \equiv 0$ or (ii) $p - \lambda c \equiv 0$. Differentiating in case (i) leads to a contradiction. Differentiating in case (ii) leads to an expression of the general form

$$\frac{d^2 H_\alpha}{dt^2} = -\alpha c^2 K f_1(p, \lambda) + f_2(p, \lambda), \tag{3.24}$$

and hence (3.23) is satisfied with $m = 1$ if the function $f_1(p, \lambda) \geq 0$. This condition is not excluded and therefore interior maximizing controls may exist along curves where $H_\alpha \equiv 0$. Such curves are known as "singular arcs".

The general nature of the optimal remains unchanged if we require $\alpha(t) \in [-1, 1]$ and thus allow the turbine to be used as a compressor over part of the wave cycle, or if we require $|\alpha(t)| \in [0, p_{cr}|p|]$ in order to ensure that the critical turbine flow rate is not exceeded. In these models the optimal control strategy is essentially 'bang-bang' with α^* taking the maximum or minimum value permitted for the control, except possibly along singular arcs.

We conclude that the optimal strategy for controlling the turbine flow is in general a 'bang-bang' strategy, but in contrast to strategies for controlling the pressure, interior controls can be optimal along singular arcs.

3.1.3 Optimal Control of Relief Valve

With the alternative mechanism where the flow is controlled using a relief valve, we have

$$q = Kp + \tilde{\alpha}\beta\sigma\sqrt{|p|}, \qquad P_A = Kp^2. \tag{3.25}$$

The optimal strategy $\tilde{\alpha}^*(t)$ must then maximize

$$-\lambda\tilde{\alpha}\beta\sigma\sqrt{|p|}, \tag{3.26}$$

and therefore

$$\begin{aligned} \tilde{\alpha}^* &= 0 \qquad \text{if } p\lambda \geq 0, \\ &= 1 \qquad \text{otherwise.} \end{aligned} \tag{3.27}$$

To prevent the flow rate exceeding the critical value at the rotational speed Ω_1, the optimal control must take the form

$$\begin{aligned} \tilde{\alpha} &= 0 \qquad \text{if } p\lambda \geq 0, \\ &= 1 \qquad \text{if } p\lambda \leq 0 \text{ and } |p| \leq p_{cr}, \\ &= \frac{|\tilde{q}| - Kp_{cr}}{\beta\sqrt{p_{cr}}} \qquad \text{otherwise.} \end{aligned} \tag{3.28}$$

In this case singular arcs can occur if either $p \equiv 0$ or $\lambda \equiv 0$. Differentiating in either case leads to a contradiction and, therefore, singular arcs are excluded and the optimal control is always 'bang-bang' in nature.

3.2 Optimal Control Strategies for Turbines with Losses

We now investigate optimal control strategies for devices with losses in the turbomachinery. The power generated at the turbine shaft is given by

$$P = qp_t\eta_t = \Omega^3\Pi\left(\frac{p_t}{\Omega^2}\right), \tag{3.29}$$

where the efficiency $\eta_t < 1$ gives a measure of the power losses. In practice the function Π is generally approximated by a symmetric quadratic form, as described in Section 2.3. A simple model of the losses in a Wells type turbine is given by

$$\Pi = K'(1 - DK')\left(\frac{p_t}{\Omega^2}\right)^2 - C. \tag{3.30}$$

where the losses depend on the parameters $D, C > 0$.

3.2.1 Control of Pressure Difference - Optimal Strategies for Turbine Losses

We model the controlled pressure either by $p_t = \alpha p$ or, in the more realistic model, by $p_t = p - \tilde{\alpha}^2\nu^2 p|p|$, and assume that the rotational speed $\Omega = \Omega_1$ is fixed. For losses of the form

(3.30), we can see that the power function P is merely scaled and shifted, and therefore the optimal control strategy remains the same as for the perfectly efficient turbine. For more general losses, where Π is the quadratic function defined in (2.23), the Maximum Principle (3.5) implies that the optimal α^* (or $\tilde{\alpha}^*$) must maximize an expression of the general form

$$p_t(\tilde{a}_2 p_t^2 + \tilde{a}_1 |p_t| - \tilde{a}_0) - \lambda c K p_t \ . \tag{3.31}$$

If $\tilde{a}_2 > 0$, this function is concave with respect to α (or $\tilde{\alpha}$) and hence the optimal control strategy must remain 'bang-bang', and no interior strategy can be maximizing.

Since the rotational speed of the turbine is assumed constant here, the flow rate $q = Kp_t$ and the efficiency $\eta_t = \eta_t(p_t)$ depend only on αp (or $\tilde{\alpha} p$). The same conclusions on the nature of the optimal control strategy must, therefore, hold for all losses where

$$K p_t [p_t \eta(p_t) - \lambda c] \tag{3.32}$$

is concave with respect to p_t. Cases where this condition doesn't hold are examined in Nichols, Falcão and Pontes (1991).

3.2.2 Control of Flow Rate - Optimal Strategies for Turbine Losses

The flow rate can be controlled either by altering the turbine flow rate, or by using a by-pass valve, or by a combination of these techniques. Power losses can be experienced now through a drop in the pressure p_t across the turbine (due to duct losses, etc.) as well as through a direct loss of power (due to mechanical losses, etc.) in the turbine. In the case of a by-pass valve, these losses affect the power output, but do not modify the form of the optimal control strategy. The optimal control remains an 'open-closed', or 'bang-bang', strategy. In the case where the flow rate through the turbine is directly controlled, however, the nature of the optimal strategies is altered significantly. This can be demonstrated by considering two simple models that illustrate the behaviour of the optimal control strategies for each type of loss in the turbomachinery.

Mechanical Losses

We assume first that the controlled flow can be written $q = K\alpha p$, where $K = K'/\Omega_1$, and that the power output is given by $P = qp\eta_t$, where the efficiency $\eta_t = 1 - \mathcal{L}/qp$ and the (mechanical) losses $\mathcal{L}$ are given by

$$\mathcal{L} = \tilde{D} q^2 + \tilde{C} = \tilde{D} K^2 \alpha^2 p^2 + \tilde{C} \tag{3.33}$$

with $\tilde{D} = \Omega_1 D$ and $\tilde{C} = \Omega_1^3 C$ at rotational speed $\Omega = \Omega_1$.

The power output is thus $P = K(\alpha p^2 - \tilde{D} K \alpha^2 p^2) + \tilde{C}$, and the Maximum Principle (3.5) implies that

$$K[\alpha p(p - \lambda c) - \tilde{D} K \alpha^2 p^2] \tag{3.34}$$

must be maximized with respect to α by the optimal strategy α^*. The gradient of the

Hamiltonian H_α satisfies

$$H_a = K[p(p-\lambda c) - 2\tilde{D}K\alpha\, p^2] = 0 \tag{3.35}$$

at

$$\alpha_M = \frac{p(p-\lambda c)}{2\tilde{D}K\,p^2}, \tag{3.36}$$

and we have

$$H_{\alpha\alpha} = -2\tilde{D}Kp^2 < 0, \quad \forall\alpha\,. \tag{3.37}$$

It follows that the optimal control $\alpha^* = \alpha_M$, provided that α_M is admissible. If we require $\alpha \in [0,1]$, then for $p(p-\lambda c) \le 0$ we must take $\alpha^* = 0$, since otherwise the expression (3.34) is negative. If $p(p-\lambda c) \ge 2\tilde{D}Kp^2$, then $\alpha_M > 1$ and α_M is not admissible. The optimal strategy is, therefore,

$$\begin{aligned} \alpha^* &= 0 \quad \text{if} \quad p(p-\lambda c) \le 0, \\ &= \alpha_M \quad \text{if} \quad 0 \le p(p-\lambda c) \le 2\tilde{D}Kp^2, \\ &= 1 \quad \text{if} \quad 2\tilde{D}Kp^2 \le p(p-\lambda c). \end{aligned} \tag{3.38}$$

Similarly, if we require $\alpha \in [-1, 1]$, then we find

$$\begin{aligned} \alpha^* &= 0 \quad \text{if} \quad p(p-\lambda c) \le -2\tilde{D}Kp^2, \\ &= a_M \quad \text{if} \quad p(p-\lambda c) \le 2\tilde{D}Kp^2, \\ &= +1 \quad \text{if} \quad 2\tilde{D}Kp^2 \le p(p-\lambda c). \end{aligned} \tag{3.39}$$

In the constrained case, where $|\alpha| \in [0, p_{cr}/|p|]$ a corresponding result holds. We have $\alpha^* = \alpha_M$ provided $|p(p-\lambda c)| \le 2\tilde{D}Kp_{cr}|p|$ and $\alpha^* = \pm p_{cr}/|p|$ otherwise, where the sign of α^* depends on the sign of $p(p-\lambda c)$.

Duct Losses

Next we examine the effect of pressure (duct) losses on the optimal control strategy. We assume again that $q = K\alpha p$ and that the power output is now given by $P = qp_t - \tilde{C}$ where p_t is approximated by $p_t = p - \alpha^2\nu^2 p|p|$. The power output is thus $P = K\alpha p(p - \alpha^2\nu^2 p|p|) - \tilde{C}$, and from the Maximum Principle (3.5) it follows that the optimal strategy α^* must maximize

$$K\left(\alpha p(p-\lambda c) - \alpha^3\nu^2 p^2|p|\right) \tag{3.40}$$

over all admissible α. The gradient H_α now satisfies

$$H_a = K\left(p(p-\lambda c) - 3\alpha^2\nu^2 p^2|p|\right) = 0 \tag{3.41}$$

at $\alpha = \pm\alpha_M$, where

$$\alpha_M = \sqrt{\frac{p(p-\lambda c)}{3\nu^2 p^2 |p|}}, \tag{3.42}$$

and we find

$$H_{\alpha\alpha} = -6\alpha\nu^2 p^2 |p| \,. \tag{3.43}$$

The Hamiltonian is therefore maximized only for $\alpha = +\alpha_M$. If we require $\alpha \in [0,1]$, then α_M is admissible for $0 \le p(p-\lambda c) \le 3\nu^2 p^2 |p|$. If $p(p-\lambda c) \le 0$, the expression (3.40) is negative for the admissible α unless $\alpha = 0$. The optimal strategy is, therefore,

$$\begin{aligned} \alpha^* &= 0 \quad \text{if} \quad p(p-\lambda c) \le 0 \\ &= \alpha^M \quad \text{if} \quad 0 \le p(p-\lambda c) \le 3\nu^2 p^2 |p| \\ &= 1 \quad \text{if} \quad 3\nu^2 p^2 |p| \le p(p-\lambda c) \,. \end{aligned} \tag{3.44}$$

If we require $\alpha \in [-1, 1]$, then $\alpha = +\alpha_M$ is admissible as before, and $\alpha = -\alpha_M$ is admissible for $-3\nu^2 p^2 |p| \le p(p-\lambda c) \le 0$, but $\alpha = -\alpha_M$ does not maximize the Hamiltonian. Since the expression (3.40) is positive for all $\alpha < 0$ if $p(p-\lambda c) \le 0$, the maximum is achieved with $\alpha = -1$ in this case. The optimal strategy is now given by

$$\begin{aligned} \alpha^* &= -1 \quad \text{if} \quad p(p-\lambda c) \le 0 \\ &= \alpha_M \quad \text{if} \quad 0 \le p(p-\lambda c) \le 3\nu^2 p^2 |p| \\ &= +1 \quad \text{if} \quad 3\nu^2 p^2 |p| \le p(p-\lambda c) \,. \end{aligned} \tag{3.45}$$

Similarly in the constrained case where $|\alpha| \in [0, p_{cr}/|p|]$ is required, we find that $\alpha^* = -p_{cr}/|p|$ for $p(p-\lambda c) \le 0$, $\alpha^* = \alpha_M$ for $0 \le p(p-\lambda c) \le 3\nu^2 p^2 |p|$ and $\alpha^* = +p_{cr}/|p|$ otherwise.

If we take a more accurate model of pressure losses, where $q = K\alpha p_t$ and $P = qp_t - \widetilde{C}$, we find that the same general results hold.

We conclude that the optimal strategy for maximizing power output in the case of simple losses in the turbomachinery is not an 'on-off', or 'bang-bang', strategy as for a perfectly efficient turbine, but interior controls must now be applied in order to obtain the optimal output. The strategy for maximizing *generated* power is therefore not the same as the strategy for *absorbing* maximum energy from the incident wave.

Although these models are not entirely realistic, the results of the analysis are typical for systems with turbine losses, and demonstrate the need for good models of the power-take-off mechanisms in order to assess the effectiveness of control strategies in wave energy devices.

4. Numerical Procedures

The analysis of Section 3 gives qualitative properties of the optimal control strategies for a generic wave energy device under various assumptions on the power-take-off and control mechanisms. In

order to determine the precise forms of the optimal controls it is necessary to apply a numerical procedure. The procedure used here consists of a constrained optimization algorithm for iteratively determining the optimal control function, together with a numerical approximation scheme for solving the state and adjoint equations.

For most of the results presented here, a projected gradient algorithm has been used to solve the optimization problem. As a class, the gradient-type algorithms have fast rates of convergence and the projected-gradient algorithm, in particular, has previously proved to be efficient for treating problems that contain singular arcs and have discontinuous solutions (Andrew, Nichols and Xu, 1990). The gradient direction is computed in this process from the state and adjoint variables (satisfying equations (3.2) and (3.4) respectively). In practice the solutions to these equations are determined approximately by a finite difference method. The iteration process is easy to implement and can be shown to converge to a solution in the neighbourhood of a local maximizer (Gruver and Sachs, 1980).

The discretized form of the projected-gradient algorithm has the advantage that the state equations are treated as strong constraints on the problem and the cost function needs only to be optimized with respect to the control variables. An alternative approach is to discretize both the cost function (3.1) and the state equation (3.2) and to treat the controls and states as independent variables. A discrete optimization technique can then be applied to determine simultaneously the optimal control and optimal state variables. This approach allows more sophisticated algorithms to be applied and can be more robust than the simpler technique we describe here, but it requires much greater computational power.

Details of the discrete form of the projected-gradient algorithm are described in the next two sections. For problems where the optimal solutions are particularly sensitive, we have also computed solutions to the fully discretized problem using the package LANCELOT (Conn, Gould and Toint, 1992).

4.1 The Projected Gradient Method

To approximate the optimal control function α that maximizes the energy functional E, given by (3.1), subject to the state equation (3.2) and the control constraints (3.3), we apply the following iterative process:

Algorithm

Step 1 : Set $E^0 := 0$, $\nabla E^0 := 0$ and $N^0 := 1$, Set $k := 1$, $s := 1$.
Choose $\alpha^0 \equiv$ constant, $\forall\ t \in [0,T]$, where $\alpha_{\min} \le \text{constant} \le \alpha_{\max}$.

Step 2: Set $\alpha^k := \alpha^{k-1} + s\nabla E^k / N^k$
If $\alpha^k < \alpha_{\min}$, set $\alpha^k := \alpha_{\min}$.
If $\alpha^k > \alpha_{\max}$, set $\alpha^k := \alpha_{\max}$.

Step 3: Solve the state equation (3.2) for $p^k = p(\alpha^k)$.

Step 4: Evaluate the functional $E^k = E(\alpha^k, p^k) \equiv \int_0^T P(\alpha^k, p^k)dt$.
If $E^k < E^{k-1}$, reduce s and goto *Step* 2.

Step 5: If $|E^k - E^{k-1}| / E^k < ETOL1$, goto *Step* 8.
If $|E^k - E^{k-1}| < ETOL2$, goto *Step* 8.

Step 6: Solve the adjoint equations (3.4) for $\lambda^k = \lambda(\alpha^k, p^k)$.

Step 7: Evaluate the functional gradient $\nabla E^k \equiv H_\alpha(\alpha^k, p^k, \lambda^k)$ and its norm $N^k = \left\|\nabla E^k\right\|$, where $H_\alpha \equiv \partial H/\partial\alpha = \partial P/\partial\alpha - \lambda c \partial q/\partial\alpha$ and H is the Hamiltonian given by (3.6).
If $k \le KTOL1$, set $k := k+1$ and goto *Step* 2 .

Step 8: STOP.

In this method the new approximation to the optimal control is chosen in *Step* 2 of each iteration as

$$\alpha^{k+1} = \mathcal{P}(\alpha^k + s\nabla E^k), \tag{4.1}$$

where $\mathcal{P}$ is the L_2 projection operator onto the set of admissible controls. Since the operator $\mathcal{P}$ has the property

$$\left\|\mathcal{P}v - v\right\|_2 = \min_{\alpha_{\min} \le \alpha \le \alpha_{\max}} \left\|\alpha - v\right\|_2, \tag{4.2}$$

it follows that the inequality

$$< \nabla E^k, \ \alpha^{k+1} - \alpha^k > \ge \frac{1}{s}\left\|\alpha^{k+1} - \alpha^k\right\|_2^2 \tag{4.3}$$

holds for the selected control α^{k+1} where $<\cdot,\cdot>$ denotes the L_2 inner product. It can be shown, therefore, that for some choice of s, $E^{k+1} > E^k$ and thus the algorithm generates a sequence of admissible controls α^k and a corresponding, monotonically non-decreasing sequence of energy functionals E^k. Provided that an optimal solution exists amongst the admissible controls, the process converges and the limiting control satisfies the necessary conditions. It may be, however, that only a local maximum is found, and it is necessary to check that the Hamiltonian H is in fact maximized by the computed solution.

The Algorithm described here defines a *function* iteration and in practice it is necessary to discretize the procedure in order to find the iterates numerically. The discretized procedure can only be shown to converge to within some neighbourhood of a true optimal solution, and the iteration may never satisfy the stopping criteria in *Step* 5 of the discretized Algorithm if the tolerences ETOL1 and ETOL2 are too small. The size of the neighbourhood of convergence depends on the step-size used in the discretization. The tolerances should depend, therefore, on this step-size and must be selected with care to ensure both the accuracy of the numerical solution and the efficiency of the computational process.

4.2 Finite Difference Approximations

In order to discretize the iteration procedure of §4.1, the interval $[0,T]$ is partitioned into n steps of length $\Delta t = T/n$ and solutions are determined at the mesh points $t_j = j\Delta t$. The state and adjoint

equations are solved using a finite difference technique and the energy functionals E^k are evaluated using a quadrature rule. The trapezoidal scheme (Lambert, 1973) is chosen to approximate the differential equations on the mesh and the functionals E^k are approximated by the trapezium rule (Johnson and Reiss, 1982). The convolution integrals in the state and adjoint equations are also approximated using the trapezium quadrature rule. The state equation for p is integrated *forward* in time from the initial condition $p(0)$, and the adjoint equation for λ is integrated in the *backward* direction from the final condition $\lambda(T)$. Both of these integrations can be shown to be absolutely stable. The schemes are also consistent and technically of order two and can be shown to converge as $h \to 0$. Since the control variable is expected to contain discontinuities, the state and adjoint variables are only expected to be piecewise smooth and, therefore, difference methods of order higher than two have no computational advantage over second order schemes.

In cases where $q(\alpha, p)$ is linear in p, the two schemes reduce to one-step *explicit* methods in the appropriate directions. If q is non-linear in p, then the difference scheme approximating the state equation for p is implicit and an inner iteration process is needed at each time step of the integration. The difference approximations to (3.2) and (3.4), in implicit form, are given by

$$\begin{aligned} & p_o = 0, \\ & p_{j+1} = p_j - \frac{c}{2}\Delta t(q_j + q_{j+1}) + \frac{c}{4}\Delta t^2 k_0(p_j + p_{j+1}) \\ & \qquad + \frac{c}{2}\Delta t^2 \sum_{i=1}^{j-1} \kappa_{j-1}(p_{i+1} + p_i) + \frac{c}{2}\Delta t(q_d(t_j) + q_d(t_{j+1})), \quad j = 0,1,\ldots n-1, \end{aligned} \tag{4.4}$$

and

$$\begin{aligned} & \lambda_n = 0, \\ & \lambda_{j-1} = \lambda_j - \frac{c}{2}\Delta t[\lambda_j \left.\frac{\partial q}{\partial p}\right|_j + \lambda_{j-1} \left.\frac{\partial q}{\partial p}\right|_{j-1} + \frac{c}{2}\Delta t^2 k_0(\lambda_j + \lambda_{j-1}) \\ & \qquad + \frac{c}{2}\Delta t^2 \sum_{j-1}^{n} \kappa_{i-j}(\lambda_i + \lambda_{i-1}) + \frac{c}{2}\Delta t\left(\left.\frac{\partial P}{\partial p}\right|_j + \left.\frac{\partial P}{\partial p}\right|_{j-1} \right), \quad j = n, n-1,\ldots 1, \end{aligned} \tag{4.5}$$

where

$$q_j = q(\alpha_j, p_j),\ \kappa_s = \kappa(s\Delta t),\ \left.\frac{\partial q}{\partial p}\right|_j = \frac{\partial q}{\partial p}(\alpha_j, p_j),\ \left.\frac{\partial P}{\partial p}\right|_j = \frac{\partial P}{\partial p}(\alpha_j, p_j),$$

and α_j, p_j, λ_j are approximations to $\alpha(t_j)$, $p(t_j)$ and $\lambda(t_j)$, respectively. The energy functional is approximated by

$$E = \Delta t(\tfrac{1}{2}P(\alpha_o, p_o) + \tfrac{1}{2}P(\alpha_n, p_n) + \sum_{j=1}^{n-1} P(\alpha_j, p_j)), \tag{4.6}$$

and the gradient ∇E at time $t = t_j$ is approximated by

$$\nabla E_j = \frac{\partial H}{\partial \alpha}(\alpha_j, p_j, \lambda_j). \tag{4.7}$$

Equation (4.5) is easily solved to give an explicit expression for λ_{j-1}. If q depends linearly on p, then equation (4.4) can similarly be solved explicitly for p_{j+1}; otherwise a fixed point iteration is needed to find p_{j+1}. The iteration takes the form

$$\begin{aligned} p_{j+1}^{0} &= p, \\ p_{j+1}^{m+1} &= (1-\frac{c}{4}\Delta t^2 \kappa_0)^{-1}(-\frac{c}{2}\Delta t q(\alpha_{j+1}, p_{j+1}^{m} + R_j), \quad m = 1,2,\ldots, \end{aligned} \tag{4.8}$$

where R_j represents all the terms in equation (4.4) that are not explicitly dependent on p_{j+1}. The iteration (4.8) defines a contraction mapping and, therefore, is convergent for a sufficiently small step-size Δt, since $\kappa_0 < 0$. The iteration is stopped when $\left| p_{j+1}^{m+1} - p_{j+1}^{m} \right| / p_{j+1}^{m+1} < PTOL$ or when the iteration parameter k exceeds a specified upper bound $KTOL2$.

4.3 Numerical Simulator

The complete discretized Algorithm described in §4.1-4.2 for solving the optimal control problem (3.1)-(3.3) is implemented in a FORTRAN program. Input required by the program includes tables of data for $\kappa(t_j)$ and $q_d(t_j)$ at discrete points $t_j = jh$. For the OWC device described in §2.2, the data for κ and q_d depends on the geometry of the device, defined by the values of a, b and h, and on the incident wave form, defined by the set of values $\{\omega_n, \mathcal{A}_n, \theta_n\}$. A subroutine is used to generate the required values of q_d and κ for given geometric and incident wave parameters (Justino, 1993). Additional input required by the program includes values for c, $\alpha_{\min}, \alpha_{\max}$ and the tolerances ETOL1, ETOL2, PTOL, KTOL1 and KTOL2. The functions $q, P, \partial q/\partial p, \partial P/\partial p, \partial q/\partial \alpha$ and $\partial P/\partial \alpha$, defining the turbine characteristics and control mechanism, are evaluated for given values of α and p by user-supplied subroutines.

The algorithm is not directly applicable to problems where the constraints on the control variable α are explicitly dependent on the state variable p. Such problems must first be transformed, as described in §3.1, and corresponding new functions q and P must be defined before the procedure can be applied.

The functions q and P used here to simulate various system models are defined as follows:

(i) QUADRATIC MODEL - pressure control with perfect efficiency:

$$q = K\alpha p, \qquad P = K\alpha^2 p^2;$$

(ii) LINEAR MODEL 1 - turbine flow rate control with perfect efficiency:

$$q = K\alpha p, \qquad P = K\alpha p^2;$$

(iii) MODEL 2 - turbine flow rate control with (mechanical) losses:

$$q = K\alpha p, \qquad P = K(\alpha p^2 - D\alpha^2 p^2 - F);$$

(iv) CONSTRAINED MODEL 2 :

$$q = K\alpha\, p, \qquad P = K(\alpha p^2 - D\alpha^2 p^2 - F), \qquad \text{for } |p| \le p_{cr},$$

$$q = K\alpha\, p_{cr}, \qquad P = K(\alpha\, p_{cr}^2 - D\alpha^2 p_{cr}^2 - F), \qquad \text{for } |p| \ge p_{cr};$$

(v) MODEL 3 - turbine flow rate control with (duct) losses:

$$q = K\alpha\, p, \qquad P = K\alpha\, p(p - \alpha^2 \nu^2 p|p|) - KF, \quad \nu^2 = DK;$$

(vi) CONSTRAINED MODEL 3 :

$$q = K\alpha\, p, \qquad P = K\alpha\, p(p - \alpha^2 \nu^2 p|p|) - KF, \qquad \text{for } |p| \le p_{cr}$$

$$q = K\alpha\, p_{cr}, \qquad P = K\alpha p_{cr}(p_{cr} - \alpha^2 \nu^2 p_{cr}|p_{cr}|) - KF, \qquad \text{for } |p| \ge p_{cr};$$

(vii) MODEL 4 - turbine flow rate control with pressure losses:

$$q = K\tilde{\alpha}(p - \tilde{\alpha}^2 \nu^2 p|p|), \qquad P = K\tilde{\alpha} p(p - 2\tilde{\alpha}^2 \nu^2 p|p| - KF;$$

(viii) MODEL 5 - by-pass valve control:

$$q = Kp + \tilde{\alpha}\beta\sigma\sqrt{|p|}, \qquad P = Kp^2;$$

5. Results and Discussion

In this final section of the report, we examine the numerical solutions to the optimal control problems formulated and analysed in Section 3. The results are computed by the methods of Section 4 for the device described in Section 2.2 and the various power-take-off and control mechanisms discussed in Sections 2.3 and 2.4. The data selected for the numerical experiments is presented first and the discussion follows.

5.1 Numerical Experiments

Numerical results are obtained for the device described in Section 2.2 for water depth $h = 10\ m$, chamber width $b = 1$ and values of $a = 15\ m$ and $a = 10\ m$. It is assumed that the device is equipped with a Wells turbine, characterised as in Section 2.3, and that the system is optimally tuned to a wave period of $10\ s$ for each value of a. The turbine constant K is thus chosen to be equal to the optimal value given by Sarmento and Falcao (1985) for a regular wave of frequency $0.1\ Hz$ incident on a device of the specified geometry. The values of the turbine constants (in $m^4\ s\ kg^{-1}$) are given by $K = 0.66 \times 10^{-3}$ for $a = 15\ m$ and by $K = 0.95 \times 10^{-3}$ for $a = 10\ m$. This device model approximates the pilot plant designed for Pico in the Azores and is close to optimal for $10\ s$ incident waves, which are typical of the wave climate at the site. The gains that are expected by controlling this system are, therefore, not great, but the numerical results are indicative of general trends.

The functions describing the power output and flow rate for the models used in the calculations are summarized in Section 4.3. In these models the turbine loss parameter F is given by $F = 0.05\, G_n^2 / K^2$, where G_n is equal to one-third of the maximum defracted flow rate $q_d(t)$ due

to a regular incident wave of frequency 0.1 Hz and amplitude 1 m. The values of F (in $kg^2\ m^{-2}\ s^{-4}$) corresponding to the values $a = 15\ m$ and $10\ m$ are thus $F = 1.94 \times 10^6$ and $F = 2.01 \times 10^6$. In Model 2, where the losses are given explicitly by expression (3.3) with $C = KF$ and $D = D/K$, the values for the loss parameter D are taken between 0.1 and 0.3. For the value $D = 0.2$ the turbine efficiency η_t is 75% at flow rate G_n and 60% at flow rate $G_n / 2$. In Model 3 the values of D are taken between 0.005 and 0.02, which is approximately equal to the maximum value for which the problem remains well-posed.

The projected gradient algorithm has been verified for various choices of the discretization step Δt and for different tolerances ETOL1 and ETOL2 defining the stopping criteria for the optimization iteration. The error tolerances are selected as functions of the discretiztion step Δt, and the algorithm is observed always to stop where the relative error tolerance is satisfied. In Table 1 the ratios of the controlled to the uncontrolled energy output for a $10\ s$ regular wave over one period are shown for different stopping criteria and different choices of $\Delta t = 10/n$, where n is the number of steps. The results are computed using Model 2 with $a = 15\ m$ and $D = 0.2$. It can be seen that the numerical solutions agree to within an error of 0.5×10^{-4}. The results shown in the subsequent Tables and in Figures 3 - 19 are computed with a step-size of $\Delta t = 10/n$, where $n = 200$, and a relative stopping criterion of ETOL1 = $7.5 \times \Delta t^2$. The order of the stopping criterion is the same as that of the truncation error of the finite difference approximations to the state and adjoint equations and of the quadrature rule for the power functional. A less accurate criterion could be applied to obtain the same accuracy in the power output, but the tighter criterion is used to ensure the accuracy of the computed control and state variables.

In Tables 2 - 11, the computed ratios of the controlled to the uncontrolled average power output are shown for the various models in the case of a incident wave with a period of $10\ s$. The results are shown for averages over the middle six periods of an optimal solution calculated over ten wave periods. The transient effects at the beginning and end of the optimization period are ignored in order to give an approximation to the average power output for an optimal periodic response. In Table 12 the same ratios are shown for an irregular wave with a typical spectrum obtained from measurements of the sea-state. In these computations the convolution integral is truncated after two periods. Experiments show that increasing the number of periods over which the optimal is calculated and/or the number of periods ignored at the ends of the interval affects the solutions only in the fifth significant figure. Increasing the number of periods retained in the memory term has slightly more effect, but the results still agree to within 2 units in the fourth significant figure. For comparison the ratios of the average controlled and uncontrolled power output over one wave period are shown in Tables 2 - 3 and Tables 8 - 9 for the different models.

The Tables show results for different sizes of devices for the different models with and without losses for incident waves of different periods. The effects of increasing losses are shown and the effects of limitations on the power-take-off. The Figures show the optimal control and the optimal response of the system for the different models defined in Section 4.3. The instantaneous optimal power output and flow rate are also shown, together with the values of the Hamiltonian and its gradient at each time step of the computation.

5.2 Discussion

From Figures 1 and 2 the optimal strategy for the control of pressure difference in a perfectly efficient device can be seen to be 'bang-bang' with periods of chattering. These results were calculated using LANCELOT (Conn, Gould and Toint, 1992). Although a local maximum of the

optimization problem has been found, it can be seen from the graph of the Hamiltonian that the optimality conditions have not been satisfied. For different initial values of the iteration, different results are obtained. All give very similar values for the optimal power output, but the onset and lengths of the periods of chattering vary slightly. The oscillations in the control occur at every discrete time step and as the number of steps in the optimization period increases, the oscillations increase.

For the control of turbine flow rate in a perfectly efficient device, the optimal strategy calculated by the projected gradient algorithm is shown in Figure 3 for one wave period of $10\ s$. It can be seen that the optimal solution contains singular arcs where the gradient of the Hamiltonian is identically zero. Over these intervals the optimal control takes interior values and, as predicted by the analysis, the optimal strategy is not 'bang-bang'. The singular arcs in this model (Model 1) can be seen to coincide roughly with the chattering periods in the pressure control model (Quadratic Model). It can be deduced that the chattering strategy is acting in practice to control the flow rate through the turbine smoothly.

In Figure 4 the turbine acts as a compressor for negative values of the control variable. It can be seen that there are relatively short periods of compression in the optimal strategy. The optimal solution again contains singular arcs, but only where the control takes positive values. From the Tables it can be seen that on average the pumping adds little useful energy to the power output. The effect increases for smaller devices relative to the wave period, but decreases with increasing (mechanical) losses. In both Figures 3 and 4 it can be observed that there is an initial surge of power where the flow rate is first switched on, and then the flow rate is cut back to conserve the pressure in the chamber in order to achieve the maximum output over the entire interval.

The optimal solutions for devices with losses in the turbomachinery (Models 2 and 3) are shown in subsequent Figures. The control strategies all contain interior solutions over part of the wave period, as predicted by the analysis of Section 3. If the conversion mechanism is allowed to act as a compressor, it is again found that the compression periods are relatively short and add relatively little to the useful power output (in comparison with the capital expenditure needed). In Figures 10 and 11 the solutions over 10 wave periods are shown. The transient effects can be observed in the first and last two of the periods. From the Tables it can be seen that the control has more effect in improving the energy output for devices that are small relative to the wave length and also that as the losses increase the control has more effect.

In Figures 7 - 9 and 15 - 17 the effects of limitations on the power-take-off are illustrated for different values of the critical pressure p_{cr}. We observe that if the critical pressure is large, the control strategy remains close to the unlimited case. As the critical pressure decreases, the control strategy gradually approaches the uncontrolled model, where the control is at its maximum, corresponding to the critical pressure value, over the whole period. From Tables 6 and 11 it is evident that the control has less effect as the limitations on the power-take-off become more stringent.

The optimal solution for a more accurate model of the turbine flow rate control mechanism (Model 4) is shown in Figure 8. The results are almost identical to those for the simple model (Model 3) and it can be concluded that the simple model gives a good approximation to the system. In Figure 19 the behaviour of the optimal strategy for controlling the by-pass valve is shown. The solution is a simple bang-bang strategy that acts simply to keep the pressure from exceeding its critical value.

Results for an irregular wave with a spectrum typical of a sea-wave are shown in Figure 12 and Table

12. The control strategy gives a good improvement to the power output, even averaged over a long time period. This improvement is dramatically increased where there are losses in the turbine.

6. Conclusions

The conclusions of the research are summarized in Section 1.1. A significant new result of these studies is that the *improvement* in the generated power produced by optimally controlling the flow rate across the turbine (independently of head difference) *increases with increasing losses* in the turbomachinery.

The results show also that the control gives greater improvement in the energy output for devices that are smaller relative to the wave length. The control of head difference across the turbine is observed to be less robust than the control of turbine flow rate (independent of head difference), and flow rate control strategies that maximize average power *output* are found to be qualitatively different from strategies that optimize energy *absorbed* from the waves.

For regular waves, if the conversion mechanism is allowed to act as a compressor, it is found that the compression periods are relatively short and that on average the pumping adds relatively little to the useful power output.

If limitations on the power-take-off are imposed so as to prevent the pressure across the turbine from exceeding its critical value, then for a large critical pressure, the control strategy remains close to the unlimited case. As the critical pressure decreases, the control strategy gradually approaches the uncontrolled model, where the control is constant over the whole period and is equal to the maximum allowable value. It is evident that the control has less effect as the limitations on the power-take-off become more stringent.

For an irregular wave with a spectrum typical of a sea-wave, the control strategy also gives a good improvement to the power output, even averaged over a long time period. This improvement is dramatically increased where there are losses in the turbomachinery.

References

[1] Andrews, T.P., Nichols, N.K. and Xu, Z. (1990) The form of optimal controllers for tidal power generation schemes. University of Reading, Department of Mathematics, Technical Report NA 8/90.

[2] Bryson, A.E. and Ho, Y.C. (1975) *Applied Optimal Control.* Halstead Press.

[3] Conn, A.R., Gould, N.I.M. and Toint, P.L. (1992) *Lancelot.* Springer-Verlag.

[4] Evans, D.V. (1982) A theory for wave-power absorption by systems of oscillating pressure distributions, *J. Fluid Mechanics*, **114**, 481 - 499.

[5] Falcao, A.F. and Justino, P.A.P. (1994) OWC wave energy devices with flow constraints. Instituto Nacional de Engenharia e Tecnologia Industrial, Lisbon. Preprint.

[6] Greenhow, M. and White, S. (1996) Control of wave energy devices. *Off-shore Wave Energy Converters (OWEC - 1)*, JOULE II - Wave Energy R & D Programme Report, Commission of the European Communities, Brussels.

[7] Greenhow, M. and Nichols, N.K. (1993) The use of time-domain models for control of OWCs, CEC DG XII JOULE Wave Energy Initiative: *Wave Energy Converters - Generic Technical Evaluation Study*, Commission of the European Communities, Brussels, Annex Report B1: Device Fundamentals/Hydodynamics, Paper 4, pp. 1 - 13.

[8] Gruver, W.A. and Sachs, E. (1980) *Algorithmic Methods in Optimal Control.* Pitman.

[9] Hoskin, R.E., Count, B.M., Nichols, N.K. and Nicol, D.A.C. (1986) Phase control for the oscillating water column. *Hydrodynamics of Ocean Wave-Energy Utilization*, (eds D.V. Evans and A.F.deO. Falcao), Springer, Berlin, 281-286.

[10] Hoskin, R.E. (1988) *Optimal Control Techniques for Wave Power Generation.* University of Reading, Department of Mathematics, PhD Thesis.

[11] Johnson, L.W. and Reiss, R.D. (1982) *Numerical Analysis* (Second Edition). Addison-Wesley.

[12] Justino, P.A.P. (1993) *Phase Control of Systems of Oscillating Water Columns for Extracting Energy from Waves*. Instituto Superior Tecnico, Technical University of Lisbon, M.E.Mech Thesis.

[13] Justino, P.A.P., Nichols, N.K. and Falcao, A.F. (1994) Optimal phase control of OWC's, *1993 European Wave Energy Symposium*, (eds. G. Elliot and G. Caratti), National Engineering Laboratory, East Kilbride, Scotland, 145 - 149.

[14] Lambert, J.D. (1973) *Computational Methods in Ordinary Differential Equations*. John Wiley & Sons.

[15] Nichols, N.K., Falcao, A.F. and Pontes, M.T. (1991) Optimal phase control of wave power devices, *Wave Energy*, Institution of Mechanical Engineers, London, 41-46.

[16] Nichols N.K. (1993) Phase control in wave energy generation, *Wave Energy R&D*, (eds. G Caratti, A.T. Lewis and D. Howett), Commission of the European Communities, Brussels, Rpt. EUR 15079, pp. 177-182.

[17] Sarmento, A.J.N.A. and Falcao, A.F. (1985) Wave generation by an oscillating surface-pressure and its application in wave energy extraction. *J. Fluid Mech.*, **150**, 467-485.

[18] Sarmento, A.J.N.A., Gato, L.M.C. and Falcao, A.F. (1990) Turbine controlled wave energy absorption by oscillating water column devices, *Ocean Engineering*, **17**, 481 - 497.

Terminology

a	device depth
A	reference area
$\mathcal{A}, \mathcal{A}_n$	wave amplitude
b	device width
$B(\omega)$, $C(\omega)$	coefficients of radiation
c	parameter $= \gamma p_a / V_0$
$C, \tilde{C}$ $D, \tilde{D}$	coefficients of power losses
E	generated energy functional
E_f	average energy flux of incident wave
∇E	gradient of E
F	coefficent of turbine loss
g	acceleration of gravity
h	channel depth
H	Hamiltonian of energy functional
i	$\sqrt{-1}$
k, k_n	wave number;
K, K'	turbine constants
L_t	turbine torque
$\mathcal{L}$	turbine losses
m	mass
n	number of finite difference steps
N	norm of ∇E
N_n	integer = ω_0 / ω_n
p	pressure difference between chamber and atmosphere
p_t	pressure difference across turbine
p_a	atmospheric pressure
p_{cr}	critical turbine pressure
P	power at turbine shaft
P_A	power available to turbine $= qp$
$\mathcal{P}$	projection operator
q	volume flow rate through the turbine
q_c	volume flow rate displaced by internal free surface
q_d	diffraction flow rate of the incident wave
q_r	radiation flow rate of the device
s	step size in gradient direction
t	time
Δt	time step
V	volume of air chamber
V_0	volume of air chamber at equilibrium
α, $\tilde{\alpha}$	control variable

α_{min}, α_{max}	lower and upper bounds on control variables
β	valve loss parameter $= A\sqrt{2/\rho_a}$
γ	specific heat ratio
η_t	turbine efficency
κ	kernel of hydrodynamic damping
λ	adjoint variable
ν	pressure loss parameter $= \rho_a K^2 / 2A^2$
Ω	rotational speed
Π	non-dimensional turbine power output
Φ	non-dimensional turbine flow rate
ρ	air density in chamber
ρ_a	atmospheric density
ρ_w	water density
σ	sign (p)
θ	phase shift of incident wave
$\omega, \omega_0, \omega_n$	angular frequency of incident wave
ξ	non-dimensional pressure variable
ξ_{cr}	critical turbine pressure

No. of steps	Tolerance			
	$0.5\ \Delta t^2$	$5\ \Delta t^2$	$7.5\ \Delta t^2$	$10\ \Delta t^2$
200	1.127532	1.127492	1.127322	1.127436
500	1.127540	1.127522	1.127522	1.127522
1000	1.127157	1.127114	1.127114	1.127114

Table 1: Comparision between step sizes and tolerances

	Without losses		With losses	
	1 period	10 periods	1 period	10 periods
Without pumping	1.062	1.035	1.127	1.075
With pumping	1.081	1.046	1.141	1.082

Table 2: Model 2, 15m device, 10s wave

	Without losses		With losses	
	1 period	10 periods	1 period	10 periods
Without pumping	1.102	1.072	1.173	1.120
With pumping	1.162	1.097	1.223	1.135

Table 3: Model 2, 10m device, 10s wave

	Wave period			
	8 sec.	10 sec.	12 sec.	15 sec.
Without losses	1.009	1.035	1.071	1.159
With losses	1.022	1.075	1.115	1.212

Table 4: Model 2, 15m device, 10s wave

	D			
	0.0	0.1	0.2	0.3
Without pumping	1.035	1.052	1.075	1.122
With pumping	1.046	1.061	1.082	1.124

Table 5: Model 2, 15m device, 10s wave, various D

	Critical pressure			
	1.0	2.0	3.0	None
Without pumping	1.000	1.050	1.073	1.075
With pumping	1.000	1.050	1.076	1.082

Table 6: Model 2, 15m device, 10s wave, lim. pressure

	Without losses		With losses	
	1 period	10 periods	1 period	10 periods
Without pumping	1.062	1.035	1.074	1.044
With pumping	1.081	1.046	1.099	1.057

Table 7: Model 3, 15m device, 10s wave

	Without losses		With losses	
	1 period	10 periods	1 period	10 periods
With pumping	1.102	1.072	1.117	1.082
Without pumping	1.162	1.097	1.187	1.110

Table 8: Model 3, 10m device, 10s wave

	Wave period			
	8 sec.	10 sec.	12 sec.	15 sec.
Without losses	1.009	1.035	1.071	1.159
With losses	1.009	1.043	1.085	1.187

Table 9: Model 3, 15m device, various waves

	D			
	0.0	0.005	0.01	0.02
Without pumping	1.035	1.042	1.044	1.050
With pumping	1.046	1.054	1.057	1.063

Table 10: Model 3, 15m device, 10s wave, various D

	Critical pressure			
	1.0	2.0	3.0	None
Without pumping	1.000	1.037	1.042	1.044
With pumping	1.000	1.037	1.050	1.057

Table 11: Model 3, 15m device, 10s wave, lim. pressure

	Run time		
Value of D	10 sec.	128 sec.	200 sec.
0.0	1.171	1.130	1.102
0.2	1.243	1.245	1.203

Table 12: Model 2. ratios of efficiencies for an irregular wave

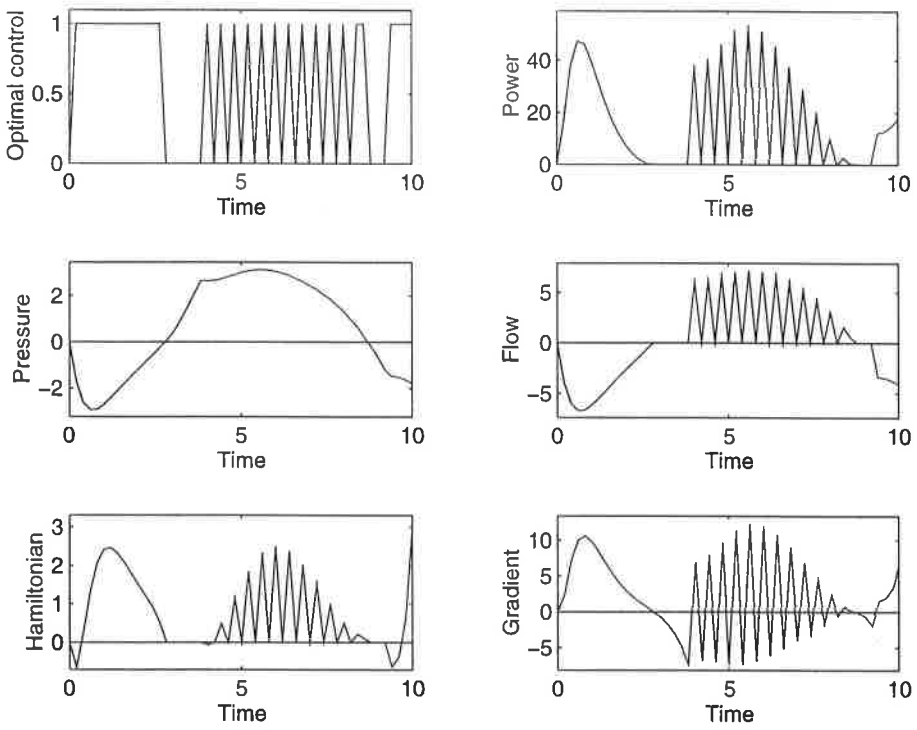

Figure 1: Quadratic model, 50 points

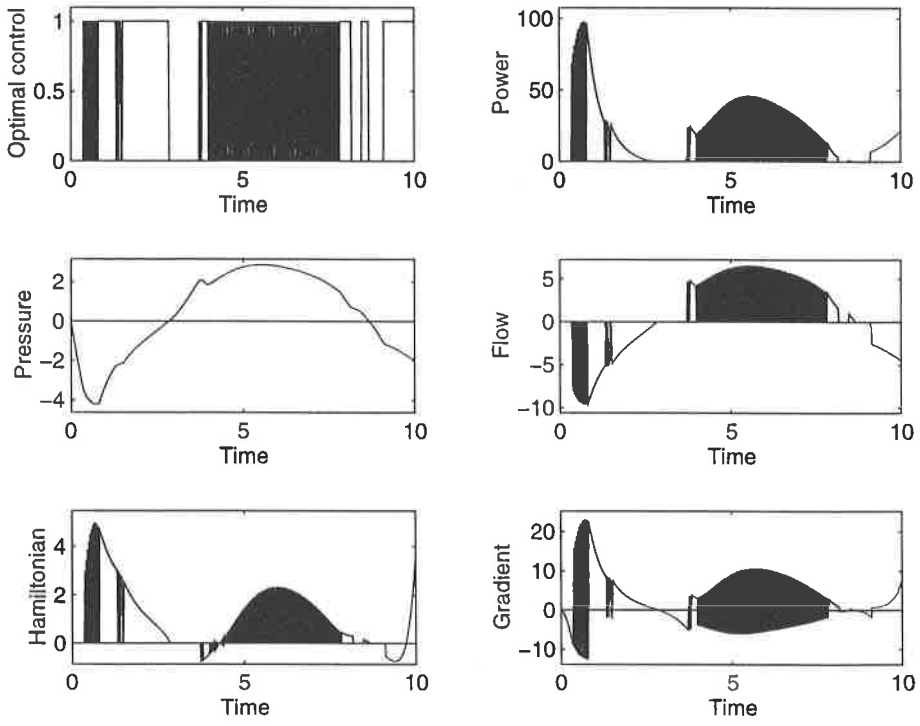

Figure 2: Quadratic model, 500 points

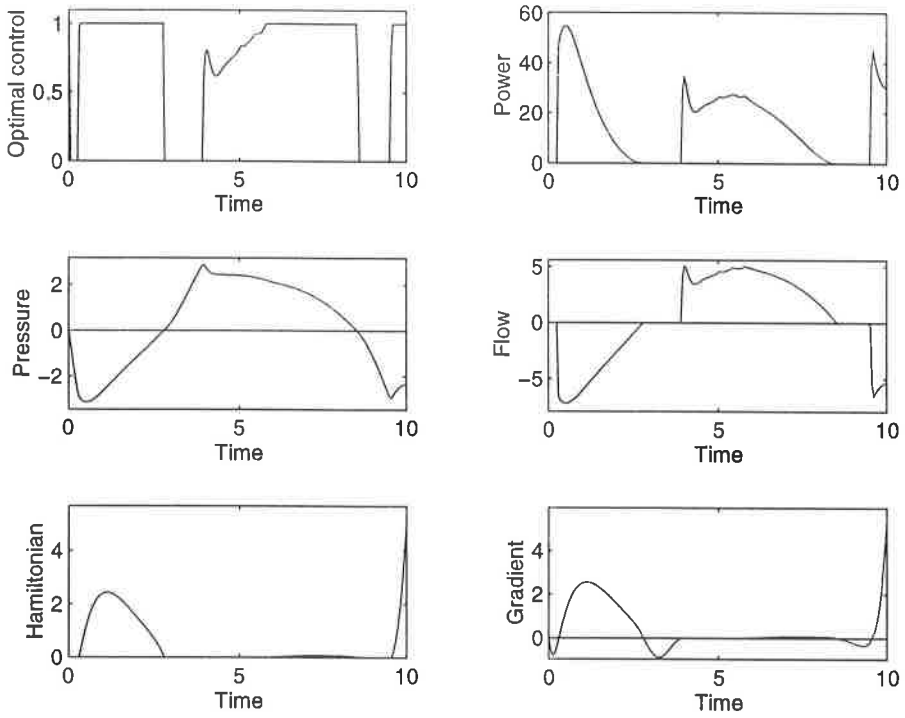

Figure 3: Model 1, without pumping

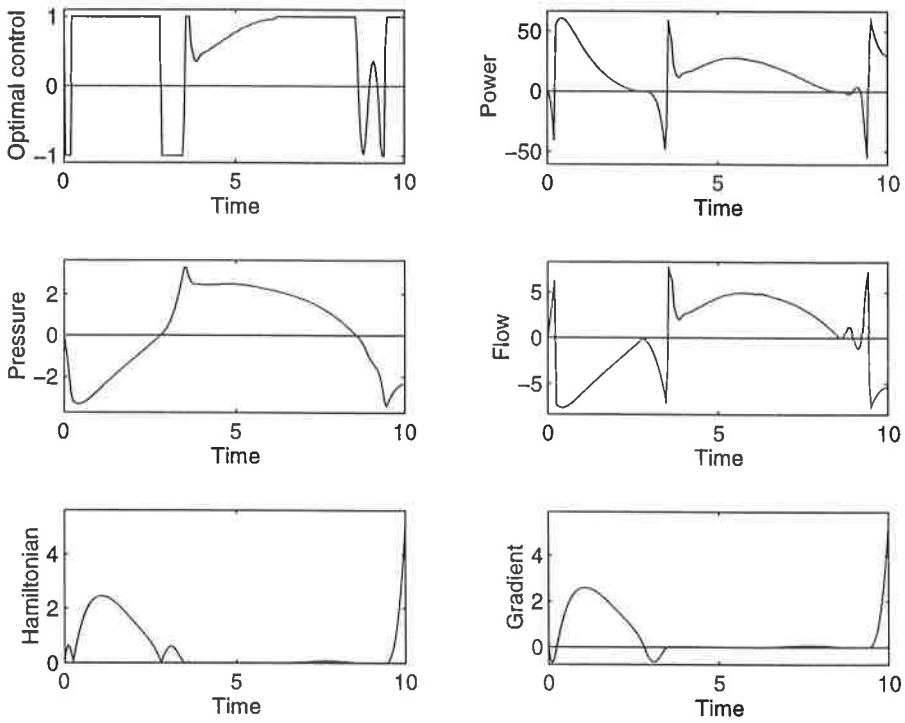

Figure 4: Model 1, with pumping

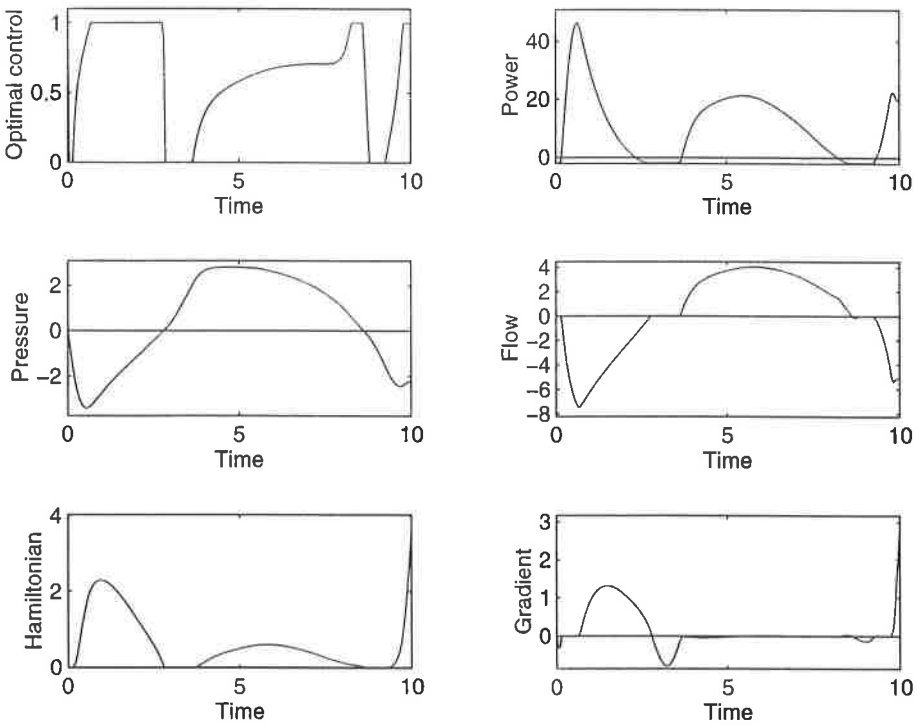

Figure 5: Model 2, without pumping, D=0.2

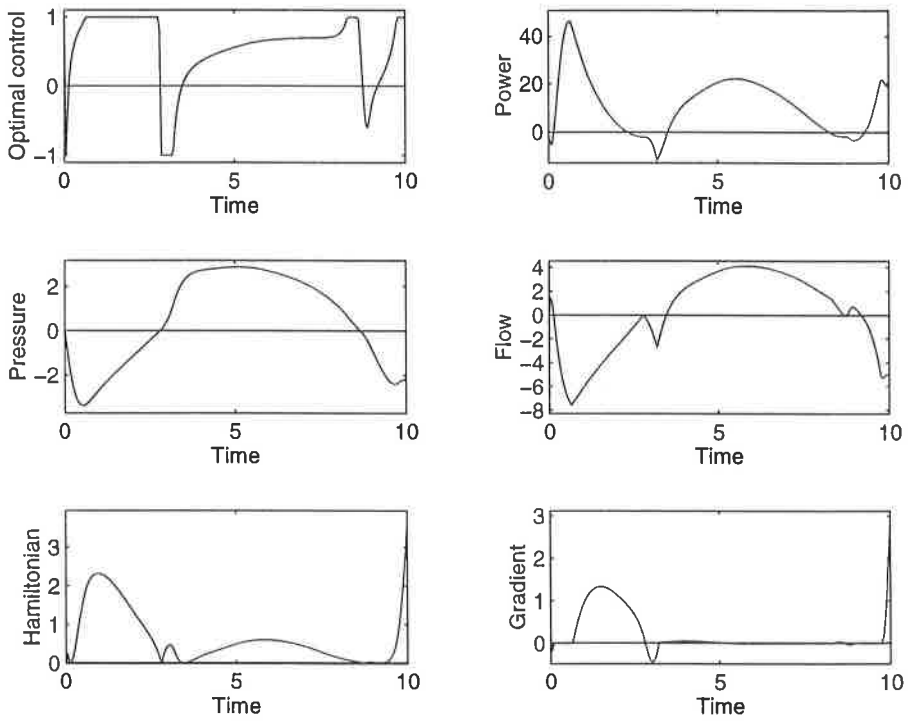

Figure 6: Model 2, with pumping, D=0.2

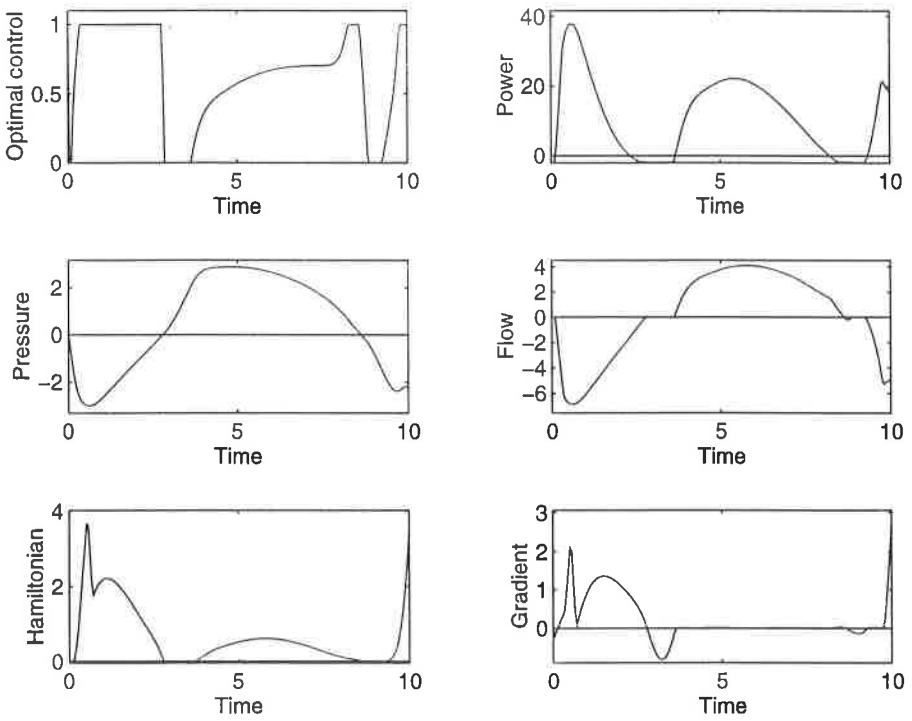

Figure 7: Model 2, D=0.2, critical pressure=3.0

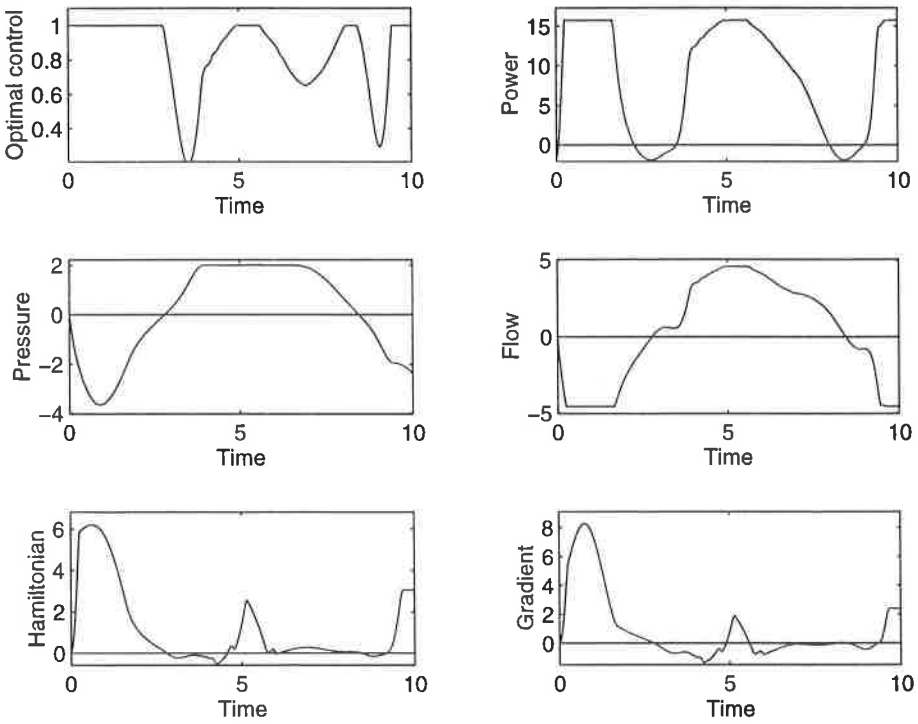

Figure 8: Model 2, D=0.2, critical pressure=2.0

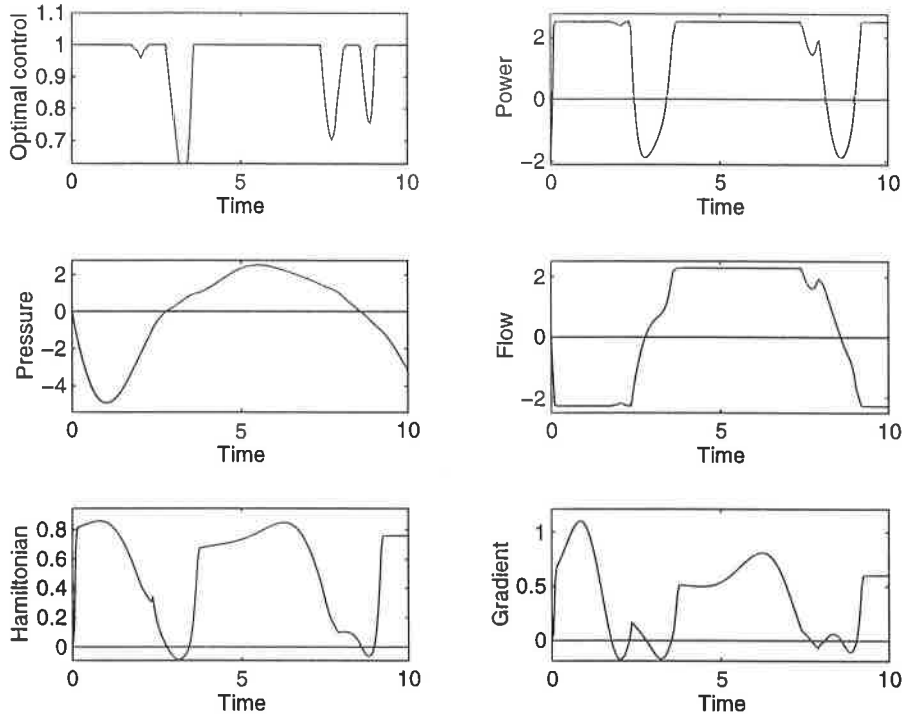

Figure 9: Model 2, D=0.2, critical pressure=1.0

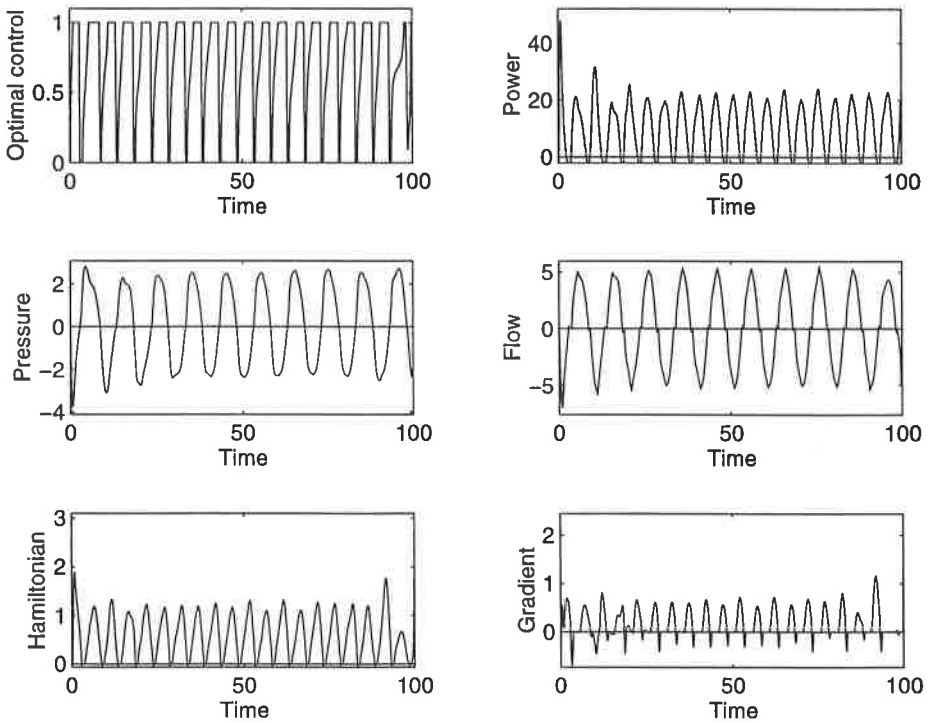

Figure 10: Model 2, 10 periods, without pumping, D=0.2

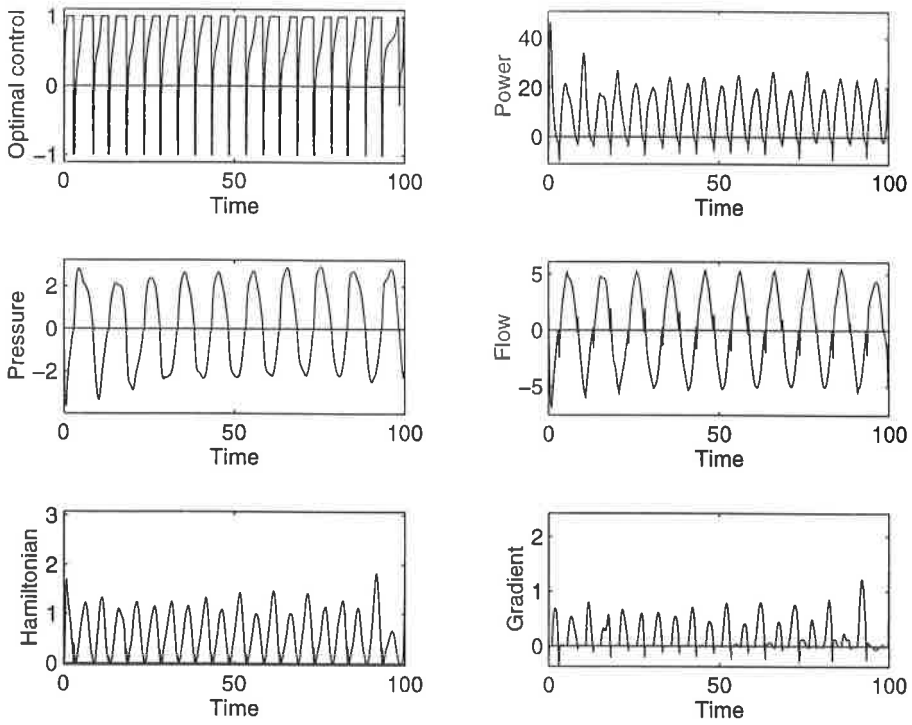

Figure 11: Model 2, 10 periods, with pumping, D=0.2

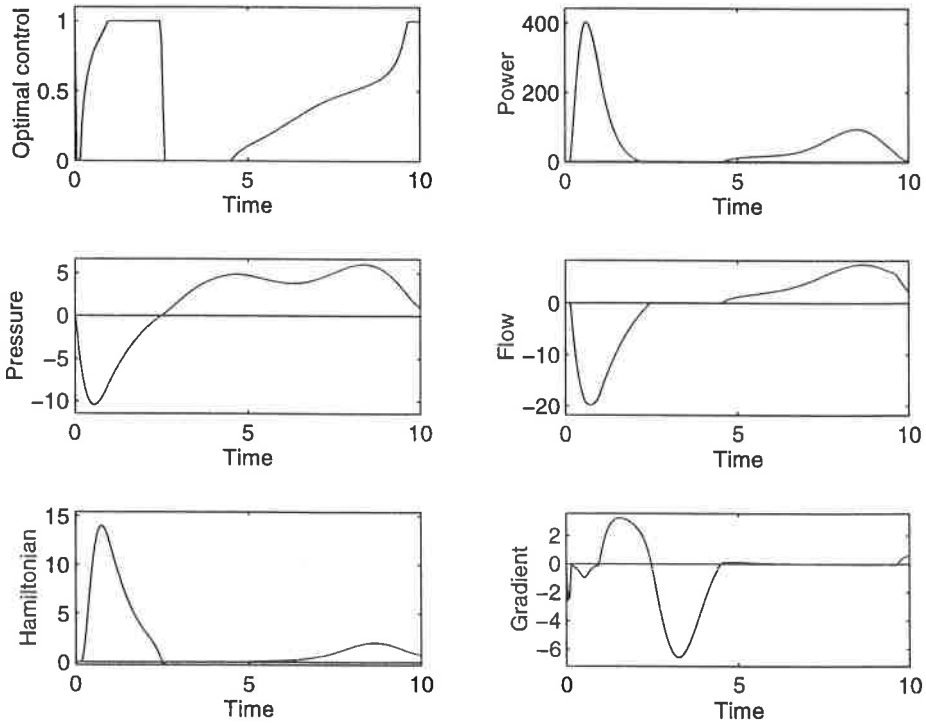

Figure 12: Model 2, irregular wave, D=0.2

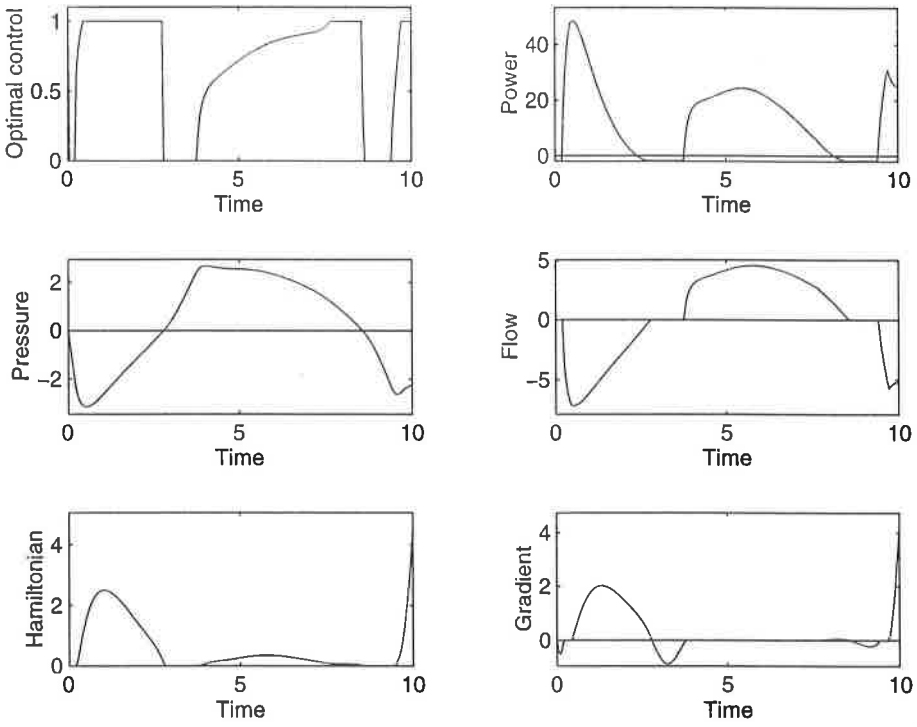

Figure 13: Model 3, without pumping, D=0.01

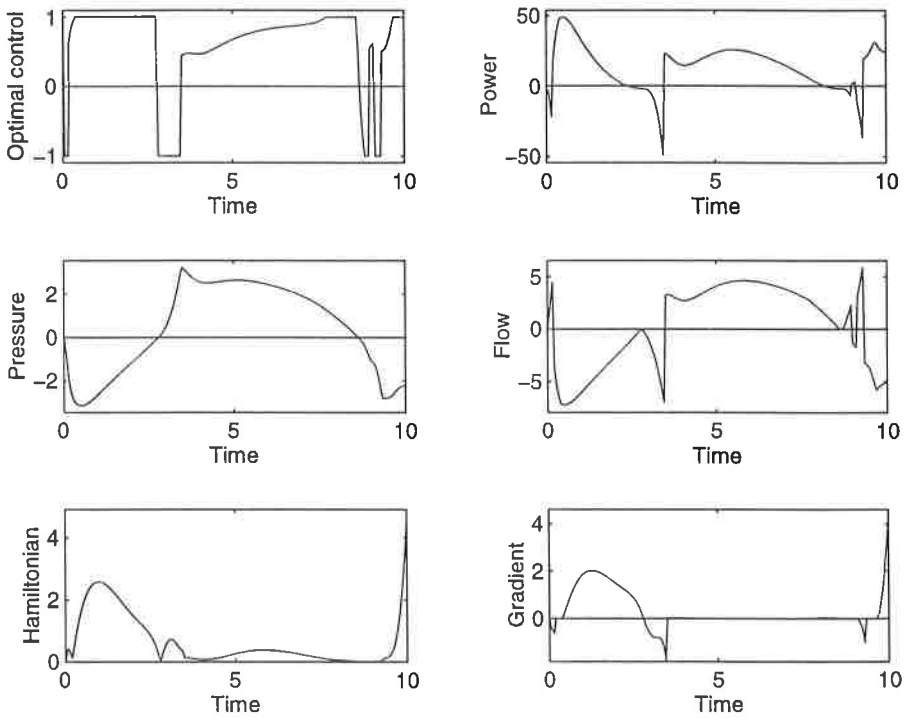

Figure 14: Model 3, with pumping, D=0.01

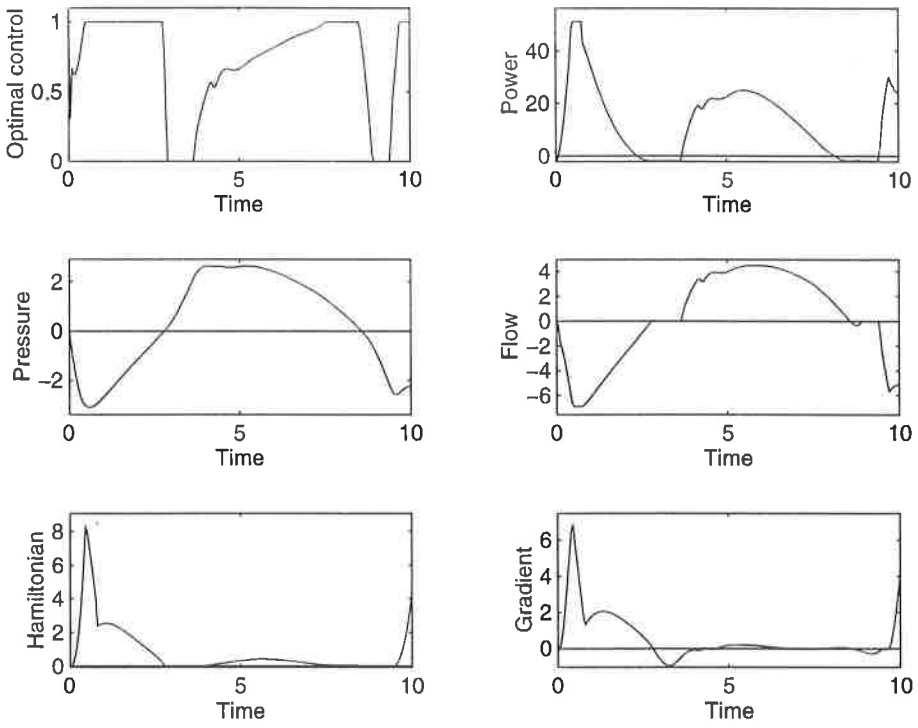

Figure 15: Model 3, D=0.01, critical pressure=3.0

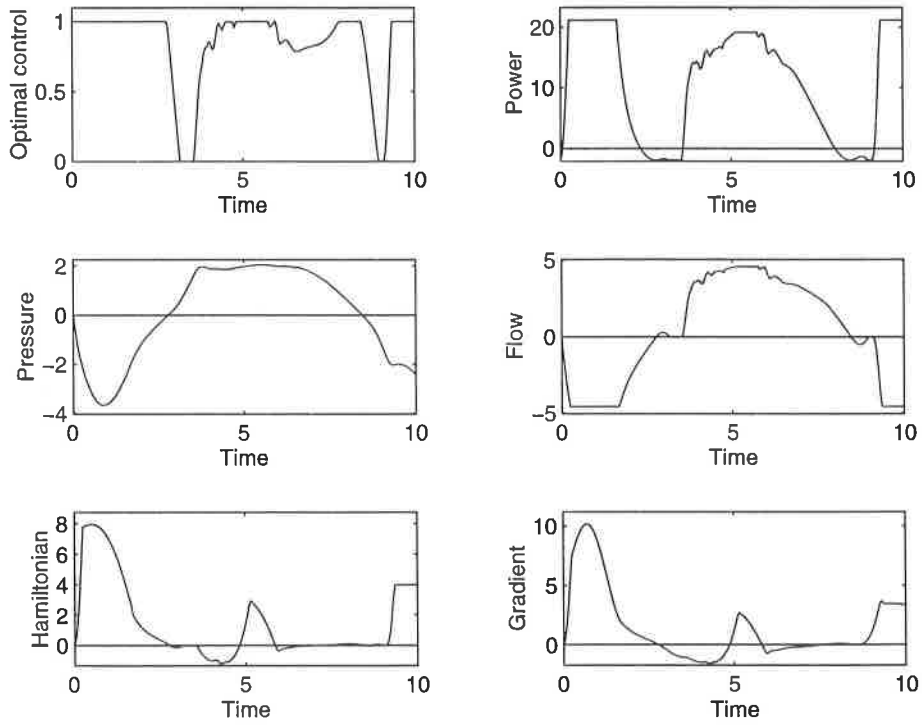

Figure 16: Model 3, D=0.01, critical pressure=2.0

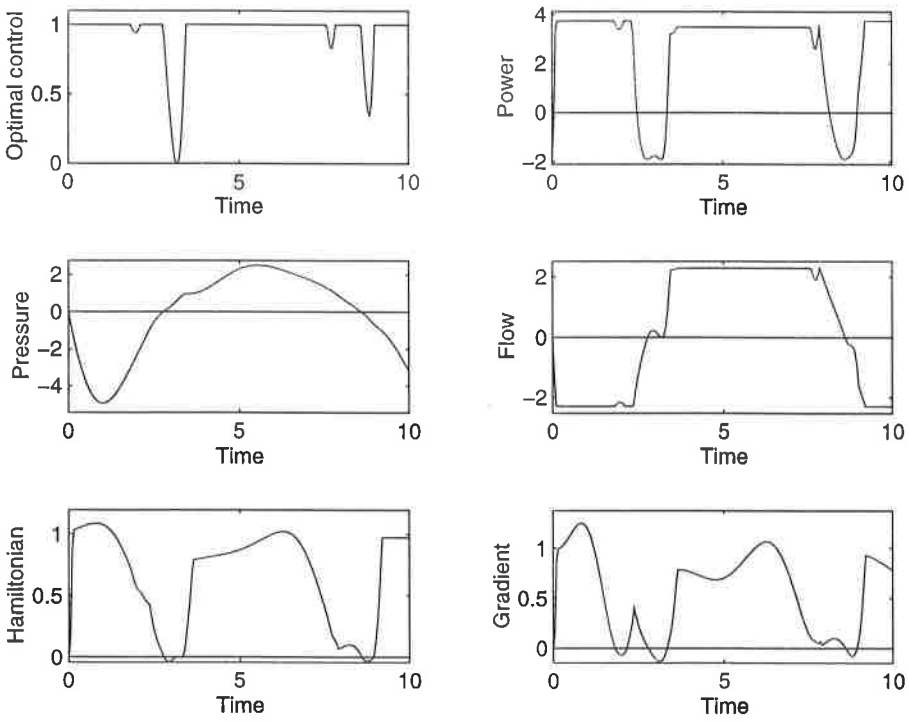

Figure 17: Model 3, D=0.01, critical pressure=1.0

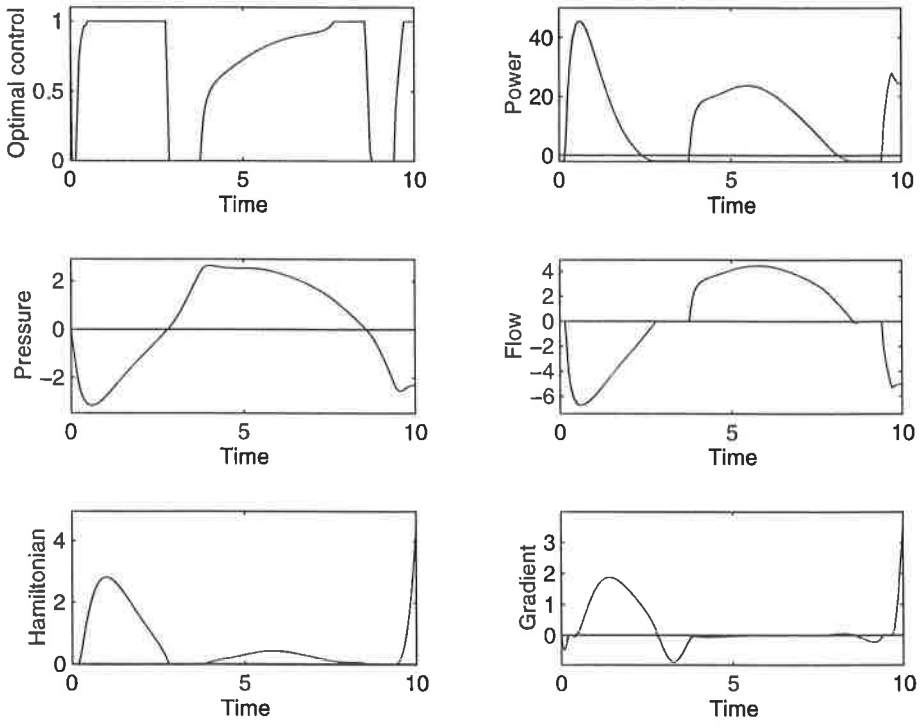

Figure 18: Model 4, D=0.01

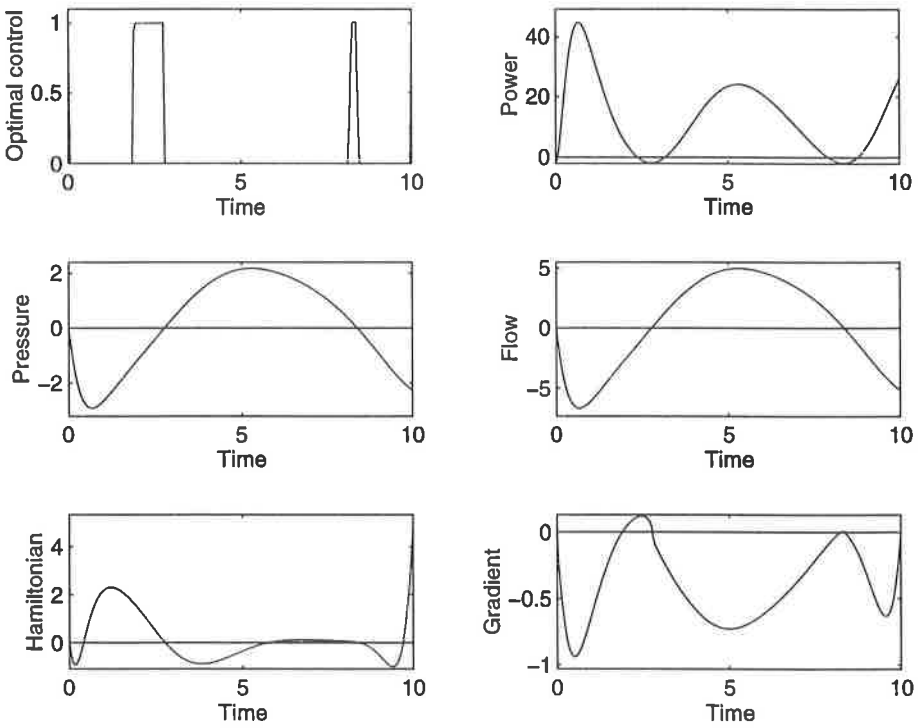

Figure 19: Model 5, D=0.01